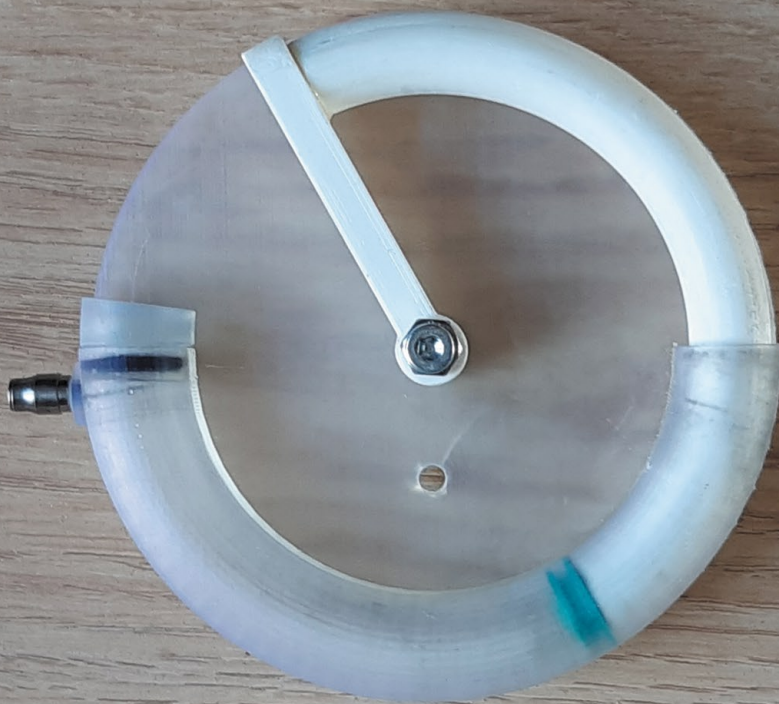


MSc thesis in Biomedical Engineering

Design and validation of a 3D printed curved hydraulic cylinder for a prosthetic wrist joint

Arine Burema
2021



Design and validation of a 3D printed curved hydraulic cylinder for a prosthetic wrist

By

A.M. Burema

in partial fulfilment of the requirements for the degree of

Master of Science
in Biomedical Engineering

with specialisation in
Biomechatronics

at the Delft University of Technology,

to be defended on Monday August 30, 2021 at 13:00u.

Thesis committee:	Prof. dr. F.C.T. van der Helm	TU Delft
	Dr. ir. D.H.Plettenburg	TU Delft
	Dr. J.Zhou	TU Delft

This thesis is confidential and cannot be made public until August 30, 2022.

An electronic version of this thesis is available at <http://repository.tudelft.nl/>.

Preface

The more you know, the more you know you don't know.
-Aristotle

When the new year starts, I will end my journey of being a student and end my journey of this graduation project. The last two years have been a journey indeed. I took my time, but that was in order to learn a lot. The first time to perform such a project is inclined to make you learn a lot about a lot of different things. This is not about the subject and all that is connected to it. The more you learn the more you know there is more to learn as well.

It has also taught me about myself and I would like to thank everybody that has supported me in this time of hard and self-discovery. All my family and friends that have supported me when things got tough or when I needed the distraction. A special thanks to Dyanne and Yasmin that have helped me by daily contact so I would feel motivated to work and by revising papers and preparing presentations. Also I would like to thank Eva and Daniel, and the other students working on their master thesis with whom I could share and talk about the struggles and learning moments during the graduation project. Further, I want to thank Dick Plettenburg, my supervisor, in guiding me through this project and for his patience when things would take longer than planned. And finally, for the technical support for designing, printing and testing the device, I would like to thank Jan van Frankenhuyzen, Spiridon van Veldhoven and Jos van Driel.

A.M.Burema
Delft, August 2021

Design and validation of a 3D printed curved hydraulic cylinder for a prosthetic wrist

Arine Burema

Abstract—Introduction: Amputees still experience problems with the use of their upper limb prostheses, mainly in the lack of comfort and functionality. This results in rejection of the prosthesis or overuse injuries due to compensatory movements. The comfort and functionality should be improved by reducing weight and increasing the degrees of freedom. The wrist is an important joint for increasing the mobility. And for reducing the weight, another actuation method than the most available and heavy electrically driven device should be used.

Methods: This study designs a hydraulic curved cylinder for the application of a wrist joint. Because of the complex and curved shape the manufacturing method used is 3D printing. The functionality of three 3D printing methods (FDM, MJF and SLA) and three sealing techniques (O-ring, X-ring, and Conus) will be evaluated by testing the amount of friction and leakage to find which configuration performs best and whether it results in an efficient actuator.

Results: The SLA-cylinders and the Conus allowed the least leakage. The combination of these two even resulted in zero leakage. For friction the SLA and FDM-cylinders performed equally, only the MJF-cylinder caused more friction. The SLA-cylinder is the only cylinder that can hold a constant pressure without leakage for 5 out of 8 pistons, when a 4 kg weight is attached. Finally, only piston-cylinder combinations with piston O-25 or Cylinder X.MJF do not match the requirements for the maximum allowed leakage and adjustment torque.

Conclusions: The piston-cylinder combination of SLA-parts and Conus perform the best. For the application of a wrist joint in prostheses more research needed for the repeatability, scalability and long-term performance.

Keywords: prosthetic wrist, hydraulic cylinder, 3D printing

I. INTRODUCTION

In the last few decades, research in the field of upper limb prosthetics has been performed to develop and improve the devices. The goal is to give people with an upper limb deficiency the functionality of their missing limb back to engage in their activities of daily living (ADL). The upper limb plays an important role in performing these ADLs. A prosthesis may help these people to live more independently and enable them to participate in society. Thus, using a prosthesis will increase their quality of life [1]. Ultimately, the aim is to give these people the functionality of a healthy human arm.

Nowadays, there are still many amputees that will not wear a prosthesis because it does not meet their needs. The rejection rates in recent studies vary from 9% to 44%, with children and above elbow amputees having higher rejection rates [1], [2]. Another study found that one third does not use their prosthesis regularly [3]. The most common (81%) reason for abandonment was limited functionality [1] and lack of comfort (70%) [2]. Other reasons given by users are high weight, difficult control, and bulkiness for electric hands [1]–[3]. But with more functionality problems arise such as increase of

weight and complexity of control. So a trade-off needs to be found between these properties.

To increase both comfort and functionality, the number of degrees of freedom (DoF) can be increased. Especially the three DoFs in the wrist are an important factor in reducing compensatory movements [4]–[6]. These are the movements made by the user to make up for the lack of DoFs in the hand and wrist. These movements are mostly found in the shoulder, elbow and trunk [4]–[6] and result in overuse injuries in the long term [7]. Reduction of these compensatory movements is an important step in improving the upper limb prosthesis.

So, while the wrist is an important joint for dexterity the influence of the wrist in prostheses has been overlooked. Most research focuses on the increase of the functionality and cosmesis of the hand. By adding degrees of freedom in the hand they provide different gripping patterns and more anthropomorphic looking hands. In upper limb prostheses only a few wrist designs are found, and most of these are passively actuated and the light weight options only provide 1 DoF [8]. To reduce the compensatory movements and increase comfort, these wrist DoFs should be increased.

Likewise, research has been focused on the development in externally powered prostheses with myo-electric control, that results in a heavy and bulky design. These factors also reduces the comfort of the prosthesis. A previous literature review found that the electrically driven prostheses are most common, see Appendix E. These devices tend to have high weight due to the presence of the motors. Thus low weight alternatives such as the hydraulic actuation without the heavy electrical elements needs more research to see if this is a plausible solution in combination with the increase of wrist dexterity.

To limit the size and weight of the wrist in the prosthesis, such a hydraulic system can be applied as a rotational actuator in the form of a curved hydraulic cylinder. This will eliminate the translation from linear to rotational movement. And with the use of coupled cylinders, no extra reservoirs are needed outside the wrist mechanism, limiting the size.

To create this curved cylinder, 3D printing should be used because this manufacturing technique is suitable for creating such complex and hollow structures. Other benefits are low costs for small quantities, customization, and light weight due to the material used [9], [10]. It is also increasingly used for building prosthetic devices. The majority of 3D printed devices is used by children, due to the benefits of customization in colours and the rapid adjustment in measurements when they grow out of it [11], [12]. Again, within the 3D printed prostheses the focus is mainly on the hand mechanism and no focus on the important wrist joint, which should be researched more. Additionally, 3D printing for actuators is little investigated,

especially for hydraulic systems. So, there lies an opportunity to explore the usability of 3D printing for hydraulics.

In sum, amputees still experience hindrance to use upper limb prostheses. Examples of hindrances were lack of functionality, resulting in compensatory movements; and discomfort due to weight. So, research should work towards a solution for these problems. Therefore, this study will design and evaluate a 3D printed curved hydraulic cylinder to find out if the combination of the manufacturing method and the actuation method result in a functional working mechanism for a prosthetic wrist joint. Specifically, the functionality of three different 3D printing methods with hydraulics will be evaluated by measuring the leakage and friction to find which configuration performs best for this application.

To make a first step, this research will focus on 1 DoF. When successful this may prove a stepping stone for the application of more DoFs and general improvement of the wrist prosthesis in the future.

II. METHODS

A. Requirements design

Requirements of the design need to be considered, such as dimensions, weight, range of motion and cut-off values for the torques. They will determine if the performance is sufficient and are based on resemblance of a human wrist joint.

The dimensions of the cylinder should be equal to the dimensions of a healthy wrist width, that has an average cross section of 50 mm [13]. But for ease of implementation a maximum of 100 mm is allowed.

The weight of the hand as percentage of the body weight varies from 0.6% to 0.9% [14]. For a person of 70 kg and using the lowest percentage this means a hand of 420 g. The wrist is just about a quarter of the size of the hand, so it should maximally weigh 100 g.

The range of motion for flexion-extension should be at least 130 degrees matching the range of motion found in a healthy wrist [15], [16]. And the range of motion for pronation-supination should be at least 150 degrees equal to the angle of healthy wrists [17], [18]. For radial and ulnar deviation a range of motion of 70 degrees is sufficient to mimic a healthy wrist [16], [18]

For the system to perform with optimum efficiency, minimal leakage is required. The goal for this system is to perform with an efficiency of 90 %, so maximal 10 % of the total volume of the cylinder is allowed to leak per rotation.

Likewise, the adjustment torques should be 0.5 Nm, which is 10% of the maximum torques people can perform. That is on average 5 Nm [19].

The static torque should be 1.5 Nm. The wrist should be able to hold an object of 2.5 kg plus the weight of a terminal device of 0.5 kg.

B. Design specifications

1) *Manufacturing methods:* For the comparison of 3D printing processes, three different processes are chosen. They are all based on a different printing principle. The first one is called Fused Deposition Modeling (FDM), this is the most



Fig. 1. The sealing options: X-ring (left), O-ring (middle), and Conus (right)

applied 3D printing method. This method is based on the principle of adding layers by molten filament extrusion from a nozzle and placing it on top of the previous layer. The second printing method is called Stereolithography Apparatus (SLA). In this printing method a liquid resin is hardened layer by layer by applying UV-light. The third method is based on the powder fusion principle, and is called Multi Jet Fusion (MJF). Here the layers are attached by a layer of powder particles and an adjacent that are heated and that way melted together. More details about these 3D printing methods can be found in Appendix A. The printing processes will have influence on the accuracy, surface roughness and alignment of the model. More accurate dimensions result in a better sealing over the whole length of the cylinder. Poor dimensional accuracy and a rough surface on the inside of the cylinder result in high friction, leakage or both. Therefore the important dimensions that have influence in the sealing performance are presented and measured using a caliper. The performance will be tested on the unprocessed cylinders straight from the printer. Because of the curved shape, post-processing is difficult and therefore disregarded.

2) *Sealing techniques:* In hydraulics, the purpose of the sealing is to eliminate leakage. The compression of the sealing ring is the most important factor of a good sealing. Other factors are the roughness of the surface in the cylinder and the permeability of the rubber sealing [20]. The compression causes a force acting on the cylinder creating a good sealing, but this force also generates friction. For this application with these small dimensions three different sealing options are available. Other sealing techniques are not applicable because the dimensions of the outer diameter were not available under 15 mm. Or they were not functional for a dynamic application, where the piston moves up and down the cylinder. The sealing techniques, Figure 1, included in this research are:

- O-ring, a widely applied sealing option, and available in a wide variety of dimensions.
- X-ring, a variation on the O-ring, with an X-shape as a cross-section, that eliminates torsion in the ring.
- Conus, a flexible cap that is used as sealing on top of the piston in a syringe.

3) *Design and dimensions:* The design for this rotational actuator is a curved cylinder with a curve of 180 degrees, see Figure 2. This results in the maximal achievable rotation of the piston. The cylinder is attached to a ground plate that connects to the other parts. It also serves for the attachment to the forearm of the prosthesis. The piston is attached to the centre of the ground plate by means of the ruler, that guides the piston to rotate around the central axis, through the cylinder. The cylinder has two open ends to make printing and removal of residual material easier. A plug closes of one

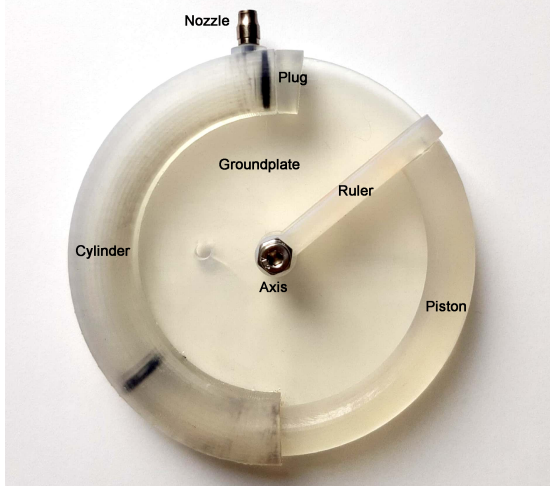


Fig. 2. The SLA model of the piston-cylinder system with the names of all the components

end of the cylinder and has the same groove to hold a sealing ring. But for a leakage free closed end this plug is glued into the cylinder. Due to the plug and thickness of the ruler the maximal rotation of the piston is 155 degrees. For fluid to enter and leave the cylinder a small opening is present at the closed end of the cylinder with a nozzle attached to connect a hose. The dimensional drawings of all the parts can be found in Appendix C.

The dimensions of the available sealing rings determine the inner diameter of the cylinders. The sealing ring the Conus has the least amount of variation in dimensions and therefore determines the dimensions for the other rings. The X-ring and Conus lack coinciding dimensions. Thus, these sealing techniques require cylinders with a different inner diameter. The dimensions for the Conus cylinder are copied from the syringe from which the Conus originates with an outer diameter of 12.5 mm. The X-ring that is closest to the outer diameter of the Conus has a diameter of 12.83 mm. So, the dimensions become 12.5 mm and 12.8 mm, for the C-cylinder for the Conus and X-cylinder for the X-ring respectively. The O-ring is available in both outer diameters of these cylinders, and therefore in both cylinders applied as a baseline. With the minimal wall thickness of 1 mm needed as design rule for all three 3D printing methods the outer diameter of the cylinder becomes 15 mm [21]–[23].

Piston diameters are based on the cylinder diameter minus 1 mm, to leave a clearance gap of 0.5 mm between the piston and the cylinder all around. The groove dimensions of the pistons are based on the design guidelines where the compression of the ring becomes 10% of the cord thickness. For dynamic applications this compression is recommended to be between 8% and 16% [20]. So, the thickness of the waist diameter determines the amount of compression of the rings. The pistons for the small O-ring (0-25) with cord thickness of 2.5 mm have a waist diameter of 8.0 mm. And piston X has a waist diameter of 8.1 mm for the X-ring and large O-ring (O-262) with cord thickness of 2.62 mm. The dimensions of the pistons for the Conus are based on the dimensions of the

TABLE I
OVERVIEW COMBINATIONS

		Piston FDM			Piston SLA		
		C	O	X	C	O	X
Cyl C	FDM	1	2	-	13	14	-
	MJF	3	4	-	15	16	-
	SLA	5	6	-	17	18	-
Cyl X	FDM	-	7	8	-	19	20
	MJF	-	9	10	-	21	22
	SLA	-	11	12	-	23	24

Conus itself and the corresponding piston from the syringe. More information about the calculations of the compression can be found in Appendix B.

C. Comparison

The comparison of the three sealing options against three printing processes, would result in nine different conditions. But due to the fact that two cylinders are needed, and the use of combining the different pistons with each cylinder, and vice versa, more combinations are formed. The overview of the combinations can be found in Table I. This ensures varying one variable to highlight its influence on the performance in the experiments. Both the influence of the printing processes and the sealing techniques can be compared separately with this method. Further, the MJF-pistons are not included for testing due to the smaller dimensions that provide insufficient sealing, see Table II. There is a piston with O-ring for both cylinders, because the O-ring is available in both dimensions that correspond to the cylinders for the other two sealing rings. The results of these two will show the repeatability of the implementation of the design rules and accuracy of the printing technique for the different dimensions. So, this study includes 24 different piston-cylinder combinations for the experiments, see Appendix D for the overview of the parts included.

D. The experiments

This study includes three different experiments to find how much leakage and friction occurs for each piston-cylinder combination. These two factors determine the efficiency of the system. The optimal performance is low friction and minimal leakage, but because they oppose each other, the goal is to find the optimum between them.

1) *Leakage test:* The first test focuses on the amount of leakage that occurs when the pistons is moved in and out of the cylinder and compare these between the different configurations. To reach the efficiency requirements of a maximum leakage of 10%, the maximum allowed leakage is 1.5 mL per rotation, as the volume of the cylinder is about 15 mL. The setup consists of a piston-cylinder combination and a syringe filled with water, connected by a tube. At the start position the syringe contains 60 mL water and the piston remains inside the cylinder. The outward motion is actuated by compressing the water in the syringe and building up the pressure in the cylinder to push the piston out. After the piston is at the end stop, outside of the cylinder, the amount of water in the syringe is noted. The inward motion is actuated by manually pushing

the piston back into the cylinder. One full rotation consists of an outward and inward rotation. When the rotation is complete, and the piston back in the cylinder, the amount of water in the syringe is measured. The rotation is repeated ten times and the average leakage per rotation is determined to compare the performance of each piston and cylinder.

2) *Friction test*: The goal of the friction test is to find the force needed to rotate the piston into the cylinder. With the pull force exerted on the ruler and piston the average adjustment torques can be calculated and provides insight in the amount of friction. Also, this test describes the consistency and magnitude of the friction force throughout the curve of the cylinder. The variation of the friction force indicates how the inner diameter of the cylinder varies, as a smaller diameter will result in higher friction.

The piston-cylinder system is attached to a tensile test bench that includes a mobile element that measures the displacement and a force sensor that measures the pull force, see Figure 3. The cylinder is attached with two screws in the wooden plate on the test bench to avoid the cylinder to rotate around the axis. The pulley attached on top of the ruler creates the translation from linear to rotational motion. The radius of the pulley r_a is 20 mm that converts the 55 mm displacement (s) limit of the tensile test bench to a rotation θ of 157 degrees, see Eq.1. This is closest to the full rotation of 155 degrees the inward motion the piston can make.

$$\theta = 360 \cdot \frac{s}{2 \cdot \pi \cdot r_a} \quad (1)$$

With the transmission of the pulley the actuation or pull force F_a remains perpendicular to the ruler, see Figure 4. Therefore the measured pull force determines the adjustment torque M_a , by multiplying it with the radius of the pulley r_a . This results in the equation

$$M_a = F_a \cdot r_a. \quad (2)$$

To eliminate other forces acting on the piston other than the friction force F_f , no water is applied in the cylinder, and the nozzle on the cylinder is not connected to a tube. This results in a free flow of air between the cylinder and surroundings. So, the pressure in the cylinder is assumed to be zero. Thus, the friction force is the only force working against the movement of the piston, causing a torque M_p on the axis. The arm r_p is the piston curve, so the torque is calculated with

$$M_p = F_f \cdot r_p. \quad (3)$$

This test setup with low velocity of the mobile element of around 1.6 mm/s causes the pull force to be the minimal force to overcome the friction, close to the equilibrium where M_p and M_a are equal. So, the magnitude of the friction force can be determined by

$$F_f = \frac{F_a \cdot r_a}{r_p}. \quad (4)$$

The arms have a constant value, r_a is 20 mm and r_p is 42.5 mm. So the friction force F_f remains a factor of 0.47 smaller than the pull force F_a .

Before the piston is placed in the cylinder it is lubricated to minimize the friction. The model with pulley on top needs to be attached by the wooden plate with the protractor in between and aligned to the curve of the cylinder, see Figure 3. The piston start position needs to be out of the cylinder with the cable wrapped around the pulley. The cable needs a little tension to stay coiled around the pulley. The starting position of the piston is at 160 degrees on the protractor. For every experiment a new Labview document is created that measures the force and displacement over time. One inward rotation is measured. For the movement of the mobile element of the test bench a wheel needs to be turned by hand, d in Figure 3. The velocity of the wheel was controlled by listening to a metronome at 70 bpm, to provide similar velocities for the mobile element. Reaching a displacement of 55 mm on the test bench ends the test. The pull force graph from the Labview document is plotted against the displacement to eliminate the influence of the velocity deviations. And the average torques and maximum torques are calculated from the average pull force and maxima in the graphs respectively.

3) *Closed system test*: This test imitates the real life situation of the joint in locked position, where no movement is allowed. The goal is to find out how much pressure is built up in the cylinder and what happens to the pressure over time. The behaviour of the pressure gives insight in the friction and leakage. The maximum angle of rotation allowed is 10 degrees during the 20 seconds the weight is applied, to reach the 90% efficiency of the system.

For this test two weight are attached to the ruler with a cord, one of 2 kg and one of 4 kg, see Figure 5 for the setup. The cylinder is attached to a wooden plate with two screws to avoid rotation around the axis and placed vertically, so the weight hangs perpendicular to the ruler and the piston is halfway inside the cylinder. The pressure build-up in the system is measured as well as the number of degrees that the piston rotates in the cylinder. In this setup both the friction and the leakage influence the pressure build-up in the system. The forces present in the cylinder can be found in Figure 6. Where F_a is the actuation force caused by the weight. The arm of the actuation r_a is 35 mm, from the axis to the place where the cord is attached to the ruler. When the piston turns away from the horizontal position, the direction of the force F_a on the ruler changes, thus changes the magnitude of the force perpendicular to the ruler that causes the rotation. The angle of rotation θ reduces the force with a factor of 0.98 for 10 degrees up to a factor of 0.87 with a rotation of 30 degrees. These changes in magnitude are small so they will be neglected. The factor of change in magnitude is calculated with

$$Factor = \frac{F_a \cdot \cos(\theta)}{F_a}. \quad (5)$$

In this setup the force on the piston F_p working against the movement and creating a torque M_p , consists of the friction force F_f and the force caused by the water pressure F_w . So, the force F_p is calculated with

$$F_p = F_f + F_w \quad (6)$$

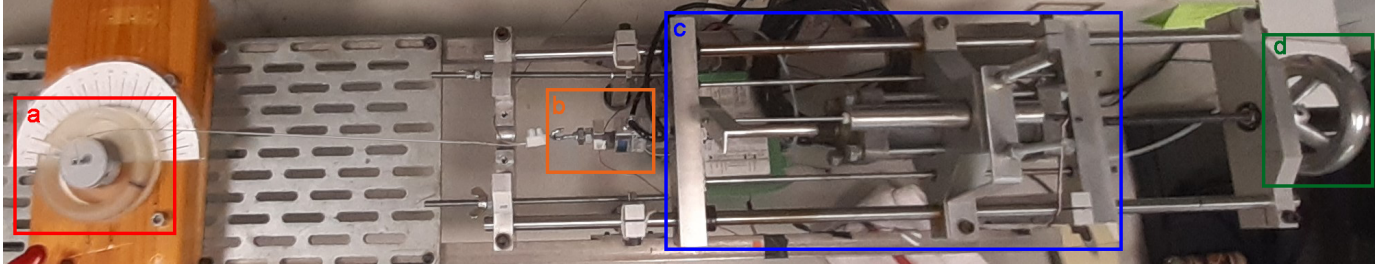


Fig. 3. Test setup for the friction test with a) the model connected to a tensile test bench with a cable. The tensile test bench consists of b) a force sensor with a hook to connect the cable, c) a mobile element with displacement sensor and d) a turning wheel for actuation. The sensors connect to a computer with Labview to document the measurements.

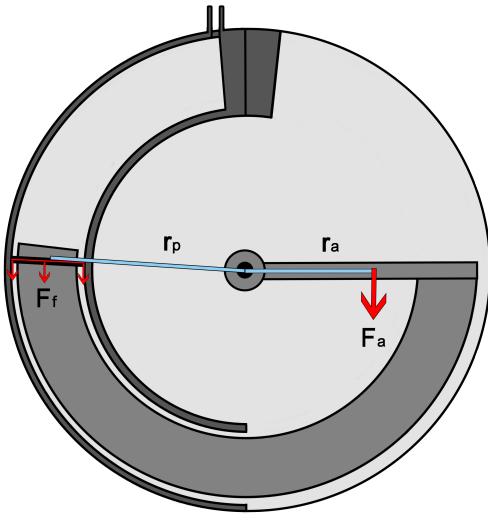


Fig. 4. Forces friction test with the friction force (F_f), the arm of the piston (r_p), the actuation force (F_a) and the arm of the actuation force (r_a)

and creates the opposing torque M_p by

$$M_p = F_p \cdot r_p. \quad (7)$$

The torque M_a caused by the actuation force F_a is calculated just as in Equation 2. The pressure force F_w caused by the pressure P_w acts on the top side of the piston. The area A_p is 123 mm^2 for the C-cylinder and 129 mm^2 for the X-cylinder. So, the force from the water pressure F_w becomes

$$F_w = A_p \cdot P_w. \quad (8)$$

In this setup the forces want to reach an equilibrium where M_a is equal to M_p . The actuation force F_a is constant so the friction force F_f and pressure development that creates the pressure force F_w are the variables that influence this equilibrium. If the pressure build-up is lacking due to leakage, force F_p is not sufficient to provide enough opposing torque M_p to reach the equilibrium and results in continuous movement of the piston. On the other hand, more friction causes a lower pressure build-up necessary to reach the equilibrium.

The starting position is at an 90 degree angle, so the piston is half inside the cylinder, which is filled with water. The valve is closed, so there is no free water flow out of the cylinder. First, the measurement program Labview starts the measurements.

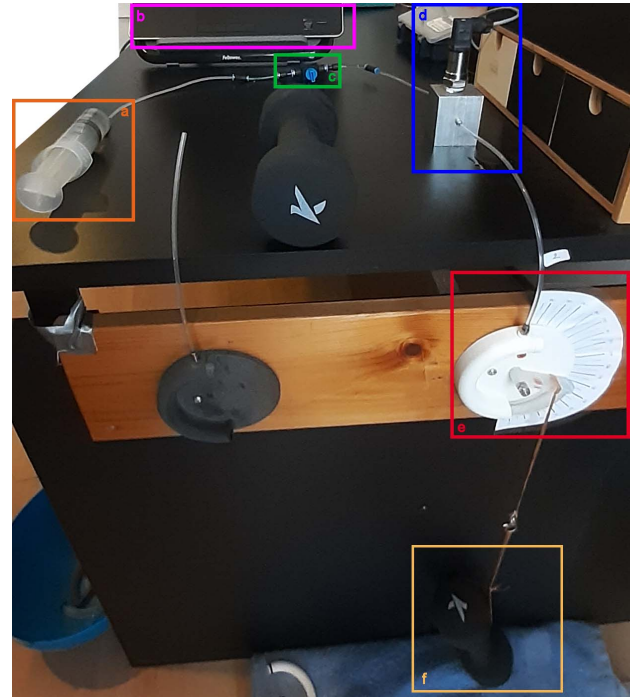


Fig. 5. Test setup for closed system test, including a) syringe, b) Laptop with Labview, c) closed valve, d) pressure sensor connected to laptop, e) piston-cylinder system, f) weight of 2 kg

After a couple of seconds the weight is attached and the timer is set for 20 seconds. When the time is up, the weight is removed from the setup and the measurements in Labview are ended.

III. RESULTS

A. Dimensions

1) *Pistons*: The dimensions of the pistons focus on the groove dimensions of the piston and the piston curve, to determine the accuracy and the alignment of the piston. They both have influence on the performance of the sealing. In Table II the original dimensions are shown, before adjustment. The dimensions larger than the goal waist diameter can be adjusted by removing the excess material, while smaller dimensions must be rejected guaranteed they will not perform sufficient. As they do not provide enough compression for a good sealing. The final groove dimensions for the pistons used in the tests

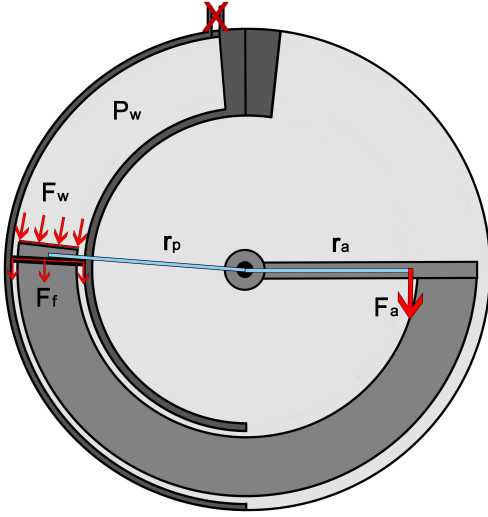


Fig. 6. The closed system test including the pressure (P_w), the force caused by the water pressure (F_w), the friction force (F_f), arm of piston (r_p), the actuation force of the cable (F_a) and the arm of actuation force (r_a)

TABLE II
INITIAL GROOVE DIMENSIONS

Piston name	Waist width [mm]	Waist height [mm]	Goal diameter [mm]
pC.SLA	7.0	7.1*	7.0
pC.FDM	7.2	7.3	7.0
pC.MJF	6.9**	6.9**	7.0
pO.SLA	8.0	8.1*	8.0
pO.FDM	8.2*	8.3*	8.0
pO.MJF	7.8**	8.1	8.0
pX.SLA	8.1	8.2*	8.1
pX.FDM	8.1	8.3*	8.1
pX.MJF	7.8**	7.9**	8.1

* adjusted
** rejected

are shown in Table III. The dimensions of the piston length and radius illustrate the accuracy error for the alignment, see Table IV.

2) *Cylinders*: The dimensions of the cylinder that are important are the inner diameters. The dimensions measured at the opening of the cylinder are shown in Table V.

B. Leakage test

1) *Pistons*: The results of the leakage per rotation is shown in Figure 7 for the C-cylinders and in Figure 8 for the X-

TABLE III
FINAL GROOVE DIMENSIONS

Piston name	Waist width [mm]	Waist height [mm]	Goal diameter [mm]
pC.SLA	7.0	7.0	7.0
pC.FDM	7.2	7.3	7.0
pO.SLA	8.0	8.0	8.0
pO.FDM	8.0	8.0	8.0
pX.SLA	8.1	8.1	8.1
pX.FDM	8.1	8.1	8.1

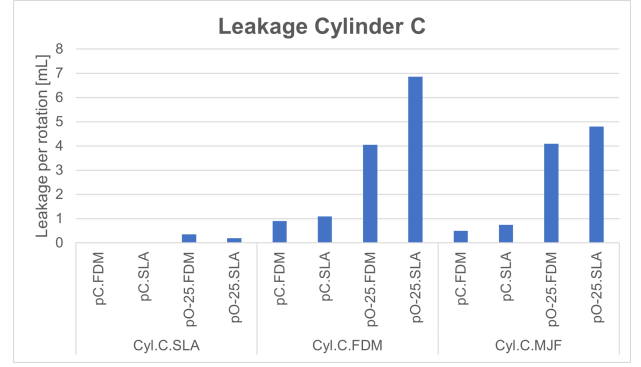


Fig. 7. Leakage per rotation in C-cylinders for the pistons C and O-25

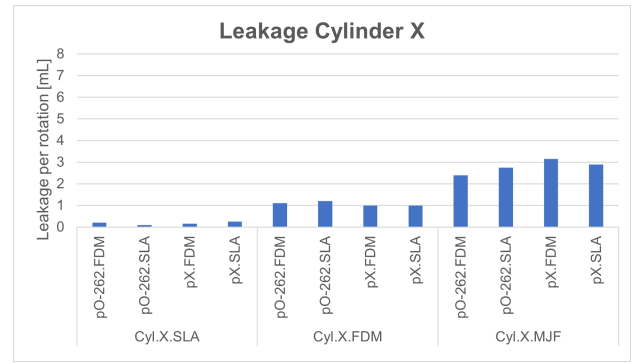


Fig. 8. Leakage per rotation in X-cylinders for the pistons X and O-262

cylinders. And the leakage of each piston averaged over the three cylinders is shown in Table VI.

2) *Cylinders*: The average leakage per rotation for every cylinder, C-cylinder and X-cylinder combined, is 1.25 mL for SLA, 17.21 mL for FDM, and 21.35 mL for MJF.

C. Friction test

1) *Pull force*: The results of the pull force needed to rotate the piston into the cylinder can be found in Figures 9 to 14. Each figure illustrates the pull force for each of the cylinders. The course of the graphs demonstrates how much force is needed throughout the curve of the cylinder. And the spikes in the graphs represent a movement with alternations in movement and stagnation. The forces for the SLA and FDM-cylinders stay between 0 N and 40 N, while the forces in the MJF-cylinder reach up to 70 N and 80 N for the X-cylinder and C-cylinder respectively.

2) *Torques*: The average and maximum torques of each piston-cylinder combination are illustrated in Figure 15 and 16. Cylinder MJF needs on average the highest average torque of 0.45 Nm and 0.57 Nm for the C-cylinder and X-cylinder respectively. It also has the highest difference between average and maximum, due to the spikes. The FDM and SLA-cylinders need on average the same amount of torque. Cylinder C.SLA needs an average of 0.22 Nm and cylinder C.FDM an average of 0.23 Nm. And cylinder X.SLA and X.FDM have an average of 0.28 Nm and 0.29 Nm respectively.

TABLE IV
PISTON LENGTH AND CURVE

Piston name	Length in print [mm]	Length in model [mm]	Radius of print [mm]	Radius of model [mm]
pC.SLA	96.3	96.5	42.3	42.5
pC.FDM	96.1	96.5	42.2	42.5
pC.MJF	96.5	96.5	42.5	42.5
pO.SLA	96.3	96.5	42.4	42.5
pO.FDM	96.1	96.5	42.2	42.5
pO.MJF	96.5	96.5	42.5	42.5
pX.SLA	96.4	96.8	42.2	42.5
pX.FDM	96.4	96.8	42.2	42.5
pX.MJF	96.8	96.8	42.5	42.5

TABLE V
INNER DIAMETERS OF CYLINDERS

		Inner diameter height [mm]	Inner diameter width [mm]	Inner diameter diagonal [mm]	Goal diameter [mm]
Cyl C	SLA	12.4	12.3	12.4	12.5
	FDM	12.5	12.5	12.4	12.5
	MJF	12.7	12.6	12.6	12.5
Cyl X	SLA	12.7	12.5	12.6	12.8
	FDM	12.8	12.7	12.6	12.8
	MJF	12.6	12.7	12.8	12.8

TABLE VI
PISTONS AND THEIR AVERAGE LEAKAGE PER ROTATION, ARRANGED FROM LEAST TO MOST LEAKAGE

Type piston	Average leakage [mL]
pC.FDM	0.47
pC.SLA	0.62
pO-262.FDM	1.23
pO-262.SLA	1.35
pX.SLA	1.38
pX.FDM	1.43
pO-25.FDM	2.83
pO-25.SLA	3.95

TABLE VII
ANGULAR ROTATION OF PISTON IN C-CYLINDERS

Piston	Weight [kg]	Angular rotation after 20 seconds [°]		
		Cyl.C.SLA	Cyl.C.FDM	Cyl.C.MJF
pC.SLA	2 kg	13	-	-
	4 kg	20	-	-
pC.FDM	2 kg	5	15	0
	4 kg	15	22	18
pO-25.SLA	2 kg	15	60	-
	4 kg	55	75	-
pO-25.FDM	2 kg	48	45	0
	4 kg	55	65	22

TABLE VIII
ANGULAR ROTATION OF PISTON IN X-CYLINDERS

Piston	Weight [kg]	Angular rotation after 20 seconds [°]		
		Cyl.X.SLA	Cyl.X.FDM	Cyl.X.MJF
pO-262.SLA	2	10	30	2
	4	18	45	-
pO-262.FDM	2	12	20	5
	4	40	50	35
pX.SLA	2	10	28	5
	4	20	45	20
pX.FDM	2	10	17	5
	4	15	47	27

D. Closed system

Figures 17 to 28 illustrate the results for the pressure development in the different piston cylinder configurations. The two conditions in weights of 2 kg and 4 kg that are attached, are shown in separate graphs for each cylinder. When the 2 kg is attached the values of the initial peak pressures lie between 0.4 bar and 0.6 bar and the pressure values for the 4 kg condition lie between 1.2 bar and 1.6 bar. And only SLA-cylinders are capable to keep the pressure constant, for 5 out of 8 piston types. Angular rotation of the piston after the 20 seconds can be found in Table VII and VIII.

E. Torques versus leakage

The results of the leakage test and the torque average of the friction test are plotted against each other. The same data is plotted, but grouped differently. Figure 29 is grouped by cylinder and Figure 30 is grouped by piston. This overview gives insight in the correlation between how much friction and how much leakage occurs in each piston cylinder configuration. For both parameters a low value is desired, so in the figures the

bottom left shows optimum performance, where there is little leakage and little torques. And wide spread in the data points of a group equals low consistency in performance.

IV. DISCUSSION

The aim was to test and evaluate hydraulic 3D printed curved cylinders. As in all new exploratory research, there were limitations in the choices that were made. Firstly, the tests and their set ups will be discussed. Thereafter, the results

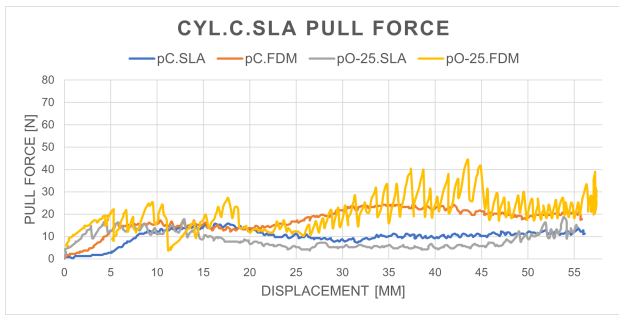


Fig. 9. The pull force of piston C and piston O-25 in Cylinder C.SLA

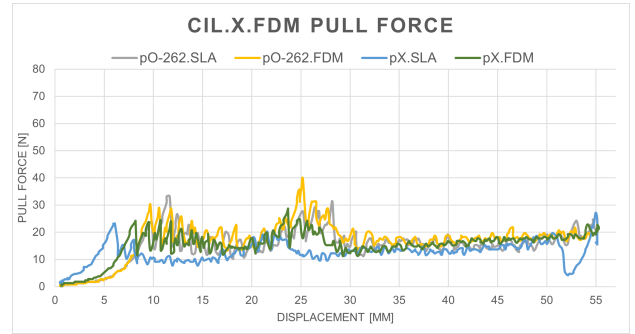


Fig. 13. The pull force of piston X and piston O-262 in Cylinder X.FDM

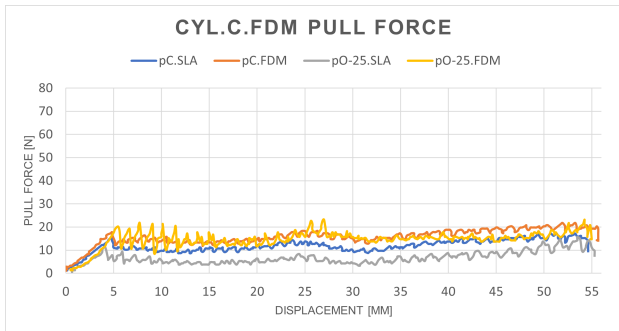


Fig. 10. The pull force of piston C and piston O-25 in Cylinder C.FDM

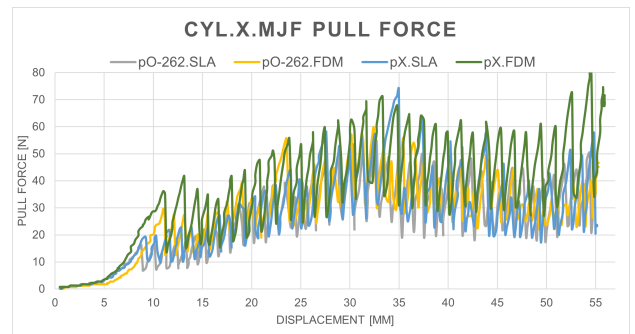


Fig. 14. The pull force of piston X and piston O-262 in Cylinder X.MJF

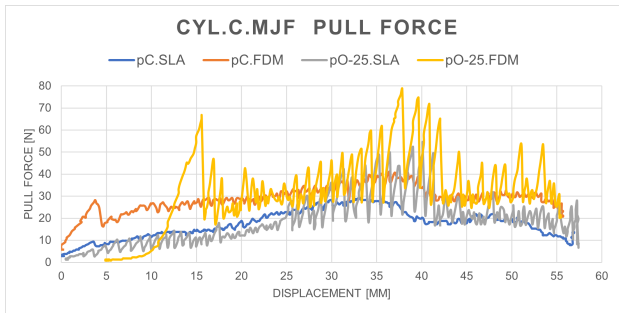


Fig. 11. The pull force of piston C and piston O-25 in Cylinder C.MJF

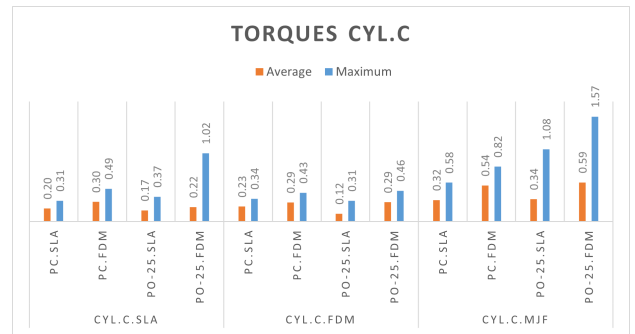


Fig. 15. Average and maximum torques for pistons in C-Cylinders

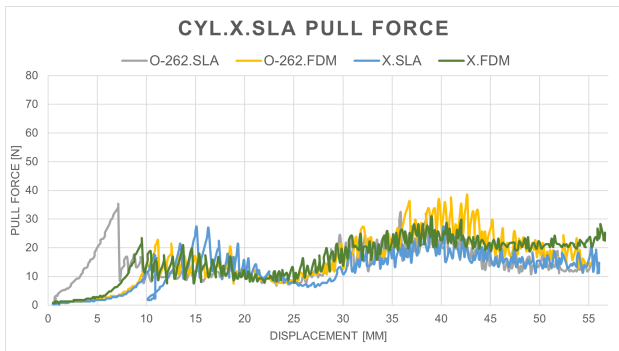


Fig. 12. The pull force of piston X and piston O-262 in Cylinder X.SLA

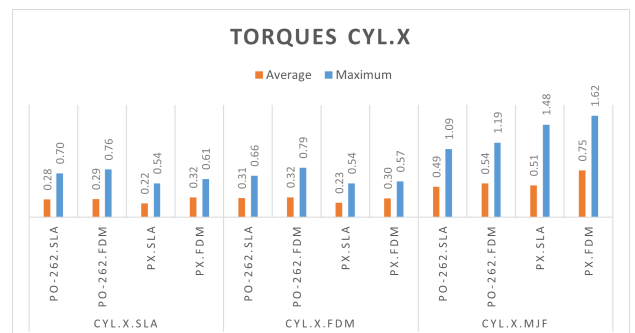


Fig. 16. Average and maximum torques for pistons in X-Cylinders



Fig. 17. Pressure development in cylinder C.SLA with a 2 kg weight attached for 20 seconds

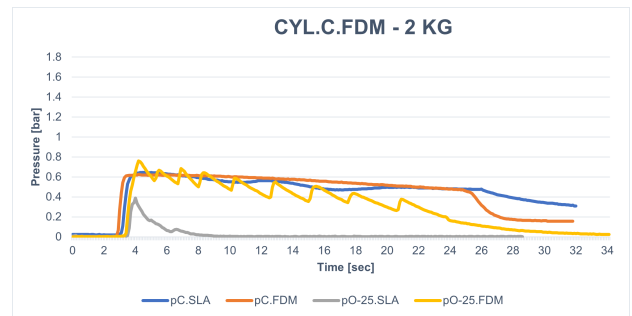


Fig. 21. Pressure development in cylinder C.FDM with a 2 kg weight attached for 20 seconds

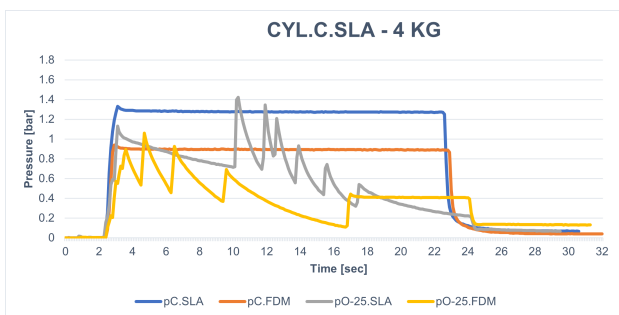


Fig. 18. Pressure development in cylinder C.SLA with a 4 kg weight attached for 20 seconds

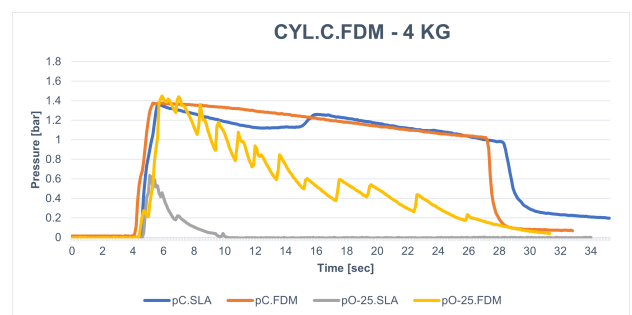


Fig. 22. Pressure development in cylinder C.FDM with a 4 kg weight attached for 20 seconds

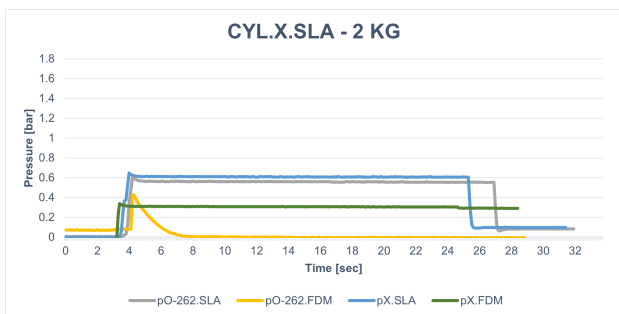


Fig. 19. Pressure development in cylinder X.SLA with a 2 kg weight attached for 20 seconds



Fig. 23. Pressure development in cylinder X.FDM with a 2 kg weight attached for 20 seconds

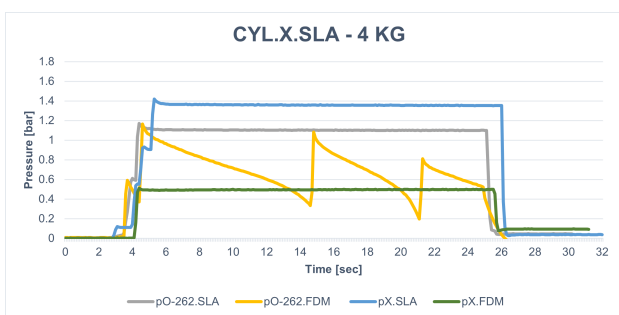


Fig. 20. Pressure development in cylinder X.SLA with a 4 kg weight attached for 20 seconds

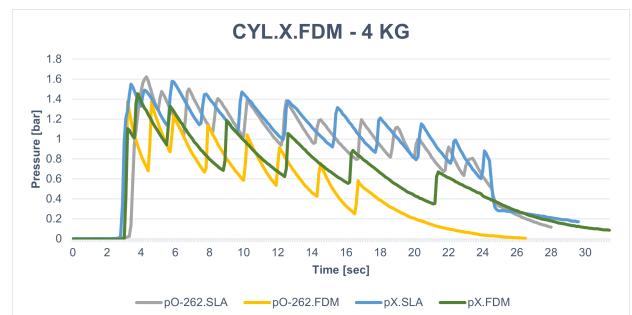


Fig. 24. Pressure development in cylinder X.FDM with a 4 kg weight attached for 20 seconds

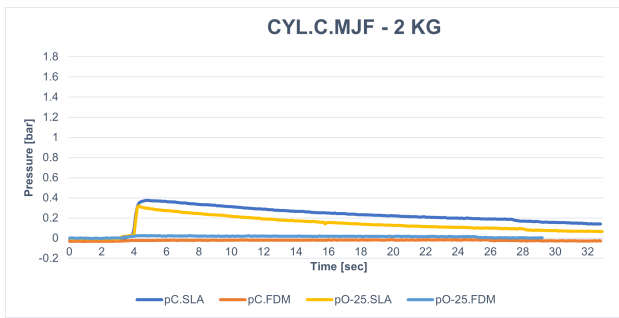


Fig. 25. Pressure development in cylinder C.MJF with a 2 kg weight attached for 20 seconds

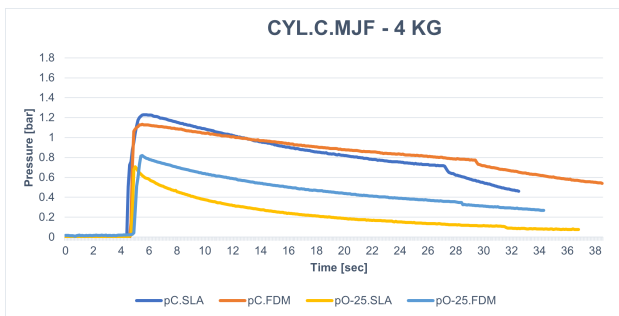


Fig. 26. Pressure development in cylinder C.MJF with a 4 kg weight attached for 20 seconds

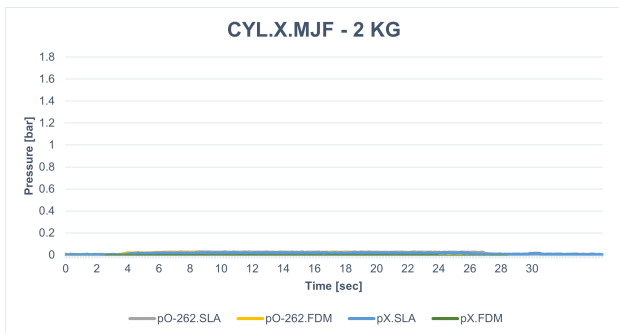


Fig. 27. Pressure development in cylinder X.MJF with a 2 kg weight attached for 20 seconds

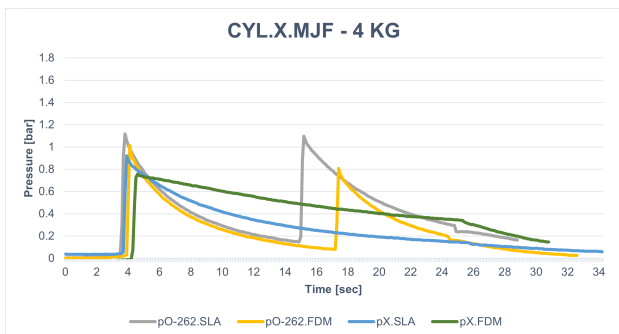


Fig. 28. Pressure development in cylinder X.MJF with a 4 kg weight attached for 20 seconds

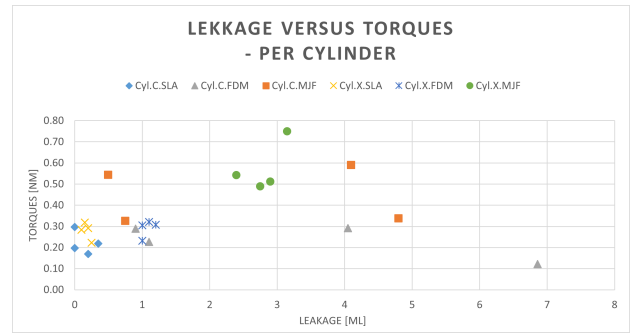


Fig. 29. Correlation of leakage versus average torques, grouped per cylinder

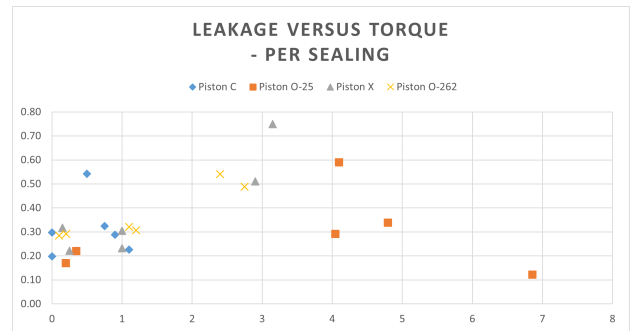


Fig. 30. Correlation of leakage versus average torques, grouped per sealing

will be set apart and interpreted, keeping these limitations in mind.

A. Evaluation initial requirements

The model used does not meet all the requirements drawn up at the start. For the ease of implementation the outer dimensions are twice the size they should be. The dimensions of the limited available sealing rings influences the diameter of the cylinder and with that the curve the cylinder can make. The 155 degrees range of motion of the piston-cylinder meets the requirements of each desired range of motion drawn up for each DoF. The piston-cylinder systems do meet the weight requirements to be below 100 g, but due to the scaling and limitation to one DoF this does not provide enough information.

B. Method limitations

1) *Design and dimensions:* To eliminate the accuracy errors for the groove dimensions the waist diameters for the O and X-pistons were altered, to obtain the right diameter and compression. However, the width of the groove was not taken into account because it was assumed that this would not influence the compression. Likewise, the dimensions of piston C.FDM were not altered, because the groove width was too small to remove the excess material with filing.

Due to the elimination of the MJF-pistons, the accurate dimensions for the alignment could not be used to determine its influence. But due to the groove dimensions being a variable as well, the influence of the alignment cannot be derived well and therefore not discussed in the results.

The dimensions of the cylinder were difficult to measure, only the inner diameter at the opening was measured. This only reflects a small proportion of the dimensions of the cylinder. The rest of the information about the dimensions of the inner diameter and the consistency throughout the curve can be collected from the friction results. Because of the relation between the inner diameter and the friction.

During the test some problems in usage of the design arised. The connection of the piston and ruler proved to be a weak point. When friction on the piston is so high to prevent movement, this creates torque in this connection that leads to fraction. This mainly happens when majority of the piston is outside of the cylinder and able to deviate from the desired rotation curve. One way to resolve this is to reduce the friction in the cylinder. Otherwise the connection needs to be strengthened, for example by printing this element as one part.

2) *Leakage test:* A limitation of the leakage test was the manual actuation. This leaves room for variation in the amount of force that is applied. Also, no information about the amount of force is collected. However, it is a good indication for how the system would be used for a real life situation, by applying enough force needed to move the piston. The actuation of the inward motion is different from the outward motion. For the inward motion the friction is overcome by the torque of the hand, while the outward motion needs to overcome the friction by the increase of pressure. But changing one of these two actuation methods leads to creating a vacuum that only works to move the piston if the sealing is sufficient. Otherwise air flows into the system through the sealing. So, the current method of actuation performs best in demonstrating the leakage.

3) *Friction test:* Here a limitation was the actuation of the tensile test bench. It was actuated manually by rotation of the actuation wheel. This way there is room for inconsistency in the velocity of the movement. In the results this influence was removed by plotting the displacement against the pull force. An alternative way to remove this error is by replacing the manual actuation by a motor with a designated velocity. Furthermore, the increase of the velocity could reduce the spikes in the graph, because it reduces the time the pull force needs to build up and overcome the friction again. Thus, the velocity of the movement should be explored to understand its influence on these factors.

The friction also causes the piston not to rotate the full angle. Because of the higher forces needed to rotate, more residual stress remains in the cable when the test bench reaches the endpoint of displacement. So, to rotate the piston with more friction the same angle, more displacement is needed. Another problem that occurs in this test setup is that the cable tension at the starting position was not equal. This results in the force to build up faster and the whole course of the graph shift to the left. This could be the case for piston X.SLA in cylinder X.FDM, where the peaks are at an earlier displacement than other pistons. Not altering the length of the cable in between measurements and checking the cable tension at the start should be able to prevent these errors. Further, the displacement should be linked to the rotation angle to get a

better insight in where exactly in the curve of the cylinder particularities such as high friction peaks occur.

4) *Closed system:* Because the direction of the actuation force on the piston changes when the angle of the piston changes, less force is applied in the direction of the rotation of the piston. This way the constant force caused by the weight decreases and does not acts as a constant force on the piston, and makes it harder to determine the other forces. So, only the pressure developments are compared, and the friction force calculations are disregarded. The translation of movement with a pully like in the friction test can be used to eliminate this.

Additionally, improvements can be made by increasing the time that the weight is attached for more long-term results. Also, the time after removing the weight can be increased, to find more information of the residual pressure in the system. Because the current results did not always reach an equilibrium in pressure at the end, which is caused by the friction at that location in the cylinder. More variations in weights or an increasing actuation force can reveal the amount of force needed for each piston to start moving. This provides more information about the friction in that piston-cylinder system that needs to be overcome.

C. Results

1) *Design and dimensions:* The performance of the hydraulic actuation depends on the sealing capabilities. And the sealing capabilities depend on the accuracy of the dimensions. The three important dimensions are the groove thickness, the piston length and curve and the cylinder inner diameters. The initial groove dimensions of the FDM-pistons are larger than the goal dimensions, and the MJF-pistons have smaller dimensions than its goal. The smaller dimensions of piston C.MJF would not influence the compression much, but for the other MJF-pistons the lower values results in insufficient compression thus insufficient sealing. So, for ease of comparison all the MJF-pistons are taken out of the comparison. The SLA-pistons have the best accuracy, only the dimensions in the waist height has an error. The waist height is in the direction of the length of the piston, which was also the printing direction. Here gravity may have played a role. So, for improving the accuracy of measurements, the different printing directions and its influence should be explored to find the optimum.

On the other hand, for the dimensions of the piston curve and length the MJF-pistons score best. So, the MJF-pistons have the best alignment. The FDM-pistons have the largest error thus the worst alignment. The errors of alignment do not reach the 1 mm error that would cause problems with the piston getting stuck in the cylinder. That only happens when the error is larger than the clearance gap of 0.5 mm on each side. The error in alignment only will cause the compression to change on the inner and outer curve of the piston. When the piston is longer than it should be, it causes the compression on the outer curve to become higher than 10%. That would result in more friction on that side. And on the inner curve the compression becomes less than the designated 10% and that causes more leakage. So, poor alignment may result in increase of both friction and leakage. However, the sealing can

compensate for this imbalance of compression and decreases the impact of the alignment on poor performance. Also, compliance of the piston-ruler element can compensate for the alignment error and reduce its influence.

The inner diameter of the SLA-cylinders are all smaller than the goal diameter, the width has the highest error. This may be caused by the fact that this is the printing direction and the gravity causing these errors. As was the case in the waist length in the SLA-pistons. All cylinder dimensions, except for cylinder C.MJF, are smaller than or equal to the goal diameter. The larger dimensions of cylinder C.MJF could cause more leakage, due to reduced compression.

2) *Leakage results:* The leakage is caused by low compression due to poor accuracy in dimensions or rough surface. The cut-off values of 1.5 mL are met in 16 out of 24 configurations. The configurations that did not meet the requirement contains piston O-25 or cylinder X.MJF. When increasing the requirement to a maximum of 0.75 mL (5%) leakage, only SLA-cylinders meet this requirement.

When comparing the sealing techniques the Conus has the least leakage, thus the best performance. This is probably due to the higher flexibility of the Conus, that has also a flexible head not constraint by the piston. It works best with a smooth surface and even reaches zero measurable leakage in the two configurations with the SLA-cylinder.

The difference between the X-ring and O-ring (O-262) is small, here the influence of the cylinder becomes more apparent than the influence of the seal. However, on average piston O-262 perform better than piston X. Due to the fact that the O-ring and X-ring have the same piston, only the seal itself is a variable within the same cylinder. O-262 only clearly performs better in the MJF-cylinder. Here the O-ring works better for the MJF-cylinder with more inner diameter variation. While the X-ring performs better for the FDM-cylinder, with a rougher surface quality.

The small O-ring (O-25) has the most leakage, caused by poor sealing performance. This could be due to the dimensions of the cylinder or the piston or the design rule influenced by the available dimensions. Firstly, the larger dimensions in the C-cylinders could cause the poor sealing, which has less influence on the Conus. Secondly, the compression for the X-cylinders is 0.3% higher, because the C-cylinders have a diameter of 12.5 mm and the O-ring (O-25) is also 12.5 mm but the design for the X-cylinder has a diameter of 12.8 mm with and 12.83 mm X-ring and O-ring (O-262). This biases the performance of the X-ring and O-262. Lastly, this design rule of the 10% compression influences the piston groove dimensions that cause poor sealing. Here the FDM-piston compensates due to the smaller width and results in less leakage. So, because these different variables all influence the compression it cannot be highlighted which of these is cause for the poor performance.

When comparing the SLA and FDM-pistons the groove dimensions and alignment are the influencing factors. In most cases, the FDM-pistons have less leakage due to the larger dimensions of the groove width. This trend is more visible in the C-cylinders than in the X-cylinders. Here, the larger dimensions of the groove, thus more compression than the

assigned 10% has a positive influence on the sealing performance. So, this influence of the compression should be explored. This could be tested using pistons with varying waist diameters that cause different amount of compression. Finally, the influence of the alignment can only be determined if it is the only variable present. In this test its influence cannot be highlighted.

From the cylinder comparison it is clear that the SLA-cylinders permit the least leakage. And the MJF-cylinders have on average the most leakage. Whereas the FDM-cylinder has the roughest surface, it performs better than MJF-cylinders. So, this would mean that the divergent diameter of the MJF-cylinder has more influence on the leakage than the rougher surface of the FDM-cylinder.

Though, within the X-cylinders the most leakage occurs in cylinder X.MJF for all pistons, in contrast cylinder C.FDM has more leakage than C.MJF for most pistons. The poor performance of cylinder C.FDM could be biased by the poor performance of piston O-25, but piston C also performs worse in this cylinder. So, the cause of this performance could be due to the rough surface of the cylinder.

The piston-cylinder combination that has the least leakage is cylinder C.SLA with piston C, which combination has zero measurable leakage. With this method it is possible to create a leak-free piston cylinder configuration.

3) *Friction results:* The comparison of the sealing techniques illustrates that the O-25 pistons have more spikes than the C pistons of the same printing technique. This difference is most apparent in cylinder C.MJF (Fig. 11). Where the difference in magnitude of the force is not equal to the increase of the spikes. So, the Conus is less prone to spikes in the graph. Possibly, this is due to the compliance or softer material of the Conus. As it is the only sealing that shows no spikes, and the only one with different material.

Further, the performance of the X and O-262 pistons are evenly matched. The only apparent outliers are the shift in the graph of piston X.SLA in cylinder X.FDM (Fig. 13) and the high peak of piston O-262.SLA in cylinder X.SLA (Fig. 12). The shift in the graph of piston X in cylinder X.FDM could be caused by a higher tension in the cable resulting in a faster force build-up and reaching the places where peaks are at an earlier displacement. To avoid these measurement errors the cable tension should be kept the same by not altering the cable length in between measurements and monitor the cable tension at the start position. The high peak of piston O-262.SLA in cylinder X.SLA could be due to an error in start position, as in the SLA-cylinder the inner diameter towards the opening becomes smaller, which causes more friction.

The FDM-pistons have on average a higher friction compared to the SLA-pistons, as a higher pull force is needed. In cylinder C.SLA the SLA-pistons even follow a different curve in the second half of the cylinder where less force is applied. They split after a displacement of 20 mm. This difference for piston C is due to the unaltered dimensions of piston C.FDM. The larger dimensions of the waist cause more compression of the Conus thus a higher friction force. For pistons X and O the groove measurements of the waist of the groove was adjusted to be equal. But the measurements of the groove width were

not taken into account. After the measurements was found that the FDM-pistons have a smaller groove width, that causes the ring to be limited in expansion when compressed between cylinder and piston. This further increases the compression and the friction caused by the compression.

Compared to the other cylinders, the FDM-cylinders have the most consistent amount of forces needed. So, these cylinders have the most consistent diameter. The highest forces occur in the MJF-cylinders, meaning this cylinder causes the most friction. The peaks in the graphs of the FDM and MJF cylinders expose that the diameter narrows and causes more friction at that point in the cylinder. For cylinder X.MJF the top of the peak is around 33 mm displacement. And in cylinder C.MJF the peak is found at a displacement between 35 mm and 40 mm, here is shown that when the pull force is higher the peak is at a higher displacement. This corresponds to the angle displacement being influenced by the friction increase as is discussed in the method review. In contrast, the curve of the pistons in the SLA-cylinders shows a force decrease around a displacement of 20 mm. This indicates a larger diameter in the middle of the curve in the SLA-cylinders.

4) *Closed system:* The amount of leakage and amount of friction both have influence on the pressure build-up in the system. Higher friction causes a lower equilibrium, initial pressure peak, and the residual pressure after the weight is removed. And the leakage is seen in the decrease of pressure, but also in the lack of pressure build-up. How fast the pressure decreases shows how much leakage occurs. And the minima of the spikes helps to explain the amount of pressure that is needed to keep the system in equilibrium and how much force is needed to overcome the friction.

The leakage causing lack of pressure build-up is only visible in the results of piston O-25.SLA in the FDM-cylinder. Here, the leakage is significant so the pressure does not build up as much as the other pistons in the same cylinder. The performance of this piston also results in significant amount of leakage and low friction in the other tests, thus has insufficient sealing.

Further, the influence of high friction on the pressure increase is clearly visible in the results of piston X.FDM in cylinder X.SLA. The equilibrium of the pressure after attaching the weight is significantly lower than other pistons in the same cylinder. The pressure does not decrease while the weight is attached, so there is no leakage. Also, after removing the weight the pressure does not decrease much. So, these deviations are caused by high friction.

The differences in piston C and piston O-25 are visible in the amount of leakage and amount of spikes. The residual pressure after the 20 seconds of piston C is always higher than the corresponding piston O-25. So, this confirms that piston C has less leakage, as was found in the leakage test. When piston C does have a decreasing pressure, less spikes occur than in piston O-25. So, just as suggested in the friction test, the spikes are caused by the hardness and thus sealing abilities of the sealing ring, as the spikes also occur for the X-ring and large O-ring (O-262). This would not create a higher friction necessarily, but less compliance of the ring for a smooth movement especially for inconsistent cylinder walls,

without stagnation. In cylinder C.MJF, piston C has a higher initial peak pressure than the O-25-piston at 4 kg, that would mean a higher friction for piston O-25. However, the results of the friction test demonstrate that the O-25 pistons do not have higher friction on average. So, it could be higher friction on that specific location in the cylinder, or be influenced by the more flexible Conus that moves through the narrow place of the MJF-cylinder more easily.

When looking at the difference between the O-262-pistons and X-pistons, the most deviating results are from piston O-262.FDM. It is the only piston that experiences leakage in the SLA-cylinder, that results in a lower peak pressure and decreasing pressure over time. Also, in the FDM-cylinder this piston reaches a lower initial peak pressure. This is not caused by increased pressure because it reveals no lower pressure in the MJF-cylinder. However it has a faster decrease in pressure, so, the deviations of this piston are caused by leakage.

The differences between the FDM and SLA-pistons can be found in cylinder X.FDM where the FDM-pistons have a faster pressure decrease. So, they have more leakage, which is the opposite of the results in the leakage test where the FDM-pistons had more leakage than the SLA-pistons. This could be caused by the fact that the closed system test does not take into account the full curve of the cylinders, which suggests more leakage for the SLA-pistons occurs at the side of the opening of the cylinder. Secondly, the pistons that do not move in cylinder C.MJF with the 2 kg attached are FDM-pistons, as no pressure build-up and no angular rotation takes place. This confirms the higher friction of the FDM-pistons due to the dimensional errors. In the other cylinders this appears as a lower initial pressure peak, especially when there is no pressure decrease. So, the trend between FDM and SLA becomes more unclear in this test. The other variables overshadow the influence of the piston type.

The comparison of the cylinders reveals that the spikes occur mostly in the FDM-cylinder. Further, only the SLA-cylinder keeps a constant pressure over time. And in de MJF-cylinder 6 out of 8 pistons do not build up any pressure. Firstly, the spikes in the FDM-cylinder could be caused by the rougher surface quality of the FDM-cylinder. That is what differentiates the FDM-cylinder from the other two. The FDM-cylinder also causes the pistons to rotate the most. The spikes occur when there is both leakage and friction present, like for piston O-25. So, the rougher surface increases both leakage and friction. Secondly, The SLA-cylinder performs best because it is the only cylinder that keeps a constant pressure over time. This is true for 6 out of 8 pistons. The pistons that do decrease are due to insufficient sealing, namely piston O-25. Finally, the lack of pressure build-up in the MJF-cylinder means the 2 kg weight is not enough to overcome the high friction forces in this spot in the cylinder. The friction test also measured forces higher than 20 N needed to move, which indicates a narrower inner diameter in the middle of the cylinder curve.

5) *Torques versus leakage:* In the plot of the leakage against the torque can be seen which configurations meet both the cut-off values for the maximal leakage of 1.5 mL per rotation and the maximum average torque of 0.5 Nm. The

piston-cylinder combinations that exceed these values mostly contain either a piston O-25 or MJF-cylinder or both. So these elements cause the system not to perform sufficiently. Overall, 15 out of the 24 configurations perform sufficiently. This overview reveals that the SLA-cylinders performs best, causing the least leakage and friction combined. The performance of the pistons presents a less clear trend, but the piston with the highest consistency is piston C. All but one combinations including this piston meet the cut-off values. This is due to the poor performance of the MJF-cylinder and the dimensional error of piston C.FDM that causes exceeding friction values.

D. Recommendation and further research

An additional static test can be performed to exclude the friction and only focus on the influence of the leakage on pressure build-up. In this setup the piston is fixated in the cylinder and the pressure is built up by flowing more water into the cylinder. This way the measured pressure is solely caused by the performance of the sealing. The drawback of this test is that only the performance of the sealing in that spot in the curve of the cylinder is measured. For more information on the whole cylinder, it needs to be repeated over different positions in the cylinder.

The next steps to improve this design are the implementation of more DoFs and scaling it down to meet the requirements of maximum dimensions of 50 mm. Also, the amount of pressure and torques the model can withstand could be increased to find out how strong it is.

The printing method proven to perform best is the SLA. However more research should be done in the repeatability and into improving the consistency of the inner diameter. Especially, the accuracy of dimensions in the printing direction should be improved. Also, the influence of the current surface roughness on life time of the sealing should be researched. As a rougher surface faster wears out the rubber of the sealing. To improve the surface quality, some smoothing techniques as possible post-processing should be investigated, while keeping in mind the accuracy of cylinders. These printing methods could also be compared to other manufacturing techniques, such as casting. The comparison of their performance on leakage and friction can result in finding the optimal way to manufacture a curved hydraulic cylinder.

V. CONCLUSION

The take-home message is:

- The majority of combinations reach the torque and leakage requirements. So, the curved cylinder is a sufficient working mechanism.
- The SLA printing technique works best for this application. In combination with most sealing techniques this printing method leads to zero leakage in the locked position in the closed system test. And only in combination with the Conus it also results in zero leakage during movement.
- The accuracy of the dimensions are the biggest problem for leakage as it is the main cause for a poor sealing performance. The varying cylinder diameter causes more

problems than a rougher surface quality. So, it is important to improve upon the consistency of the cylinder diameter. The other critical dimensions that needs to be controlled are the groove dimensions that provide the compression of the sealing ring. This dimension also needs to be optimized. Varying the compression by adjusting these dimensions within the suitable range could help find the optimal compression for minimal friction and leakage.

- The current piston-cylinder system is a suitable working mechanism, but there is still improvement needed on tolerances, long-term performance, repeatability of printing and scalability of the model.

REFERENCES

- [1] M. Yamamoto, K. Chung, J. Sterbenz, M. Shauver, H. Tanaka, T. Nakamura, J. Oba, T. Chin, and H. Hirata, "Cross-sectional international multicenter study on quality of life and reasons for abandonment of upper limb prostheses," *Plastic and Reconstructive Surgery - Global Open*, vol. 7, p. 1, 05 2019.
- [2] S. Salminger, H. Stino, L. H. Pichler, C. Gstoettner, A. Sturma, J. A. Mayer, M. Szivak, and O. C. Aszmann, "Current rates of prosthetic usage in upper-limb amputees have innovations had an impact on device acceptance?" *Disability and Rehabilitation*, vol. 0, no. 0, pp. 1–12, 2020, pMID: 33377803. [Online]. Available: <https://doi.org/10.1080/09638288.2020.1866684>
- [3] E. Biddiss, D. Beaton, and T. Chau, "Consumer design priorities for upper limb prosthetics," *Disability and rehabilitation. Assistive technology*, vol. 2, pp. 346–57, 12 2007.
- [4] T. Bertels, T. Schmalz, and E. Ludwigs, "Objectifying the functional advantages of prosthetic wrist flexion." *JPO: Journal of Prosthetics and Orthotics*, vol. 21, pp. 74–78, 04 2009.
- [5] S. Carey, M. Highsmith, and R. Dubey, "Range of motion of upper limb joint angles during two tasks for transradial prosthetic design," 01 2007.
- [6] A. Hussaini and P. Kyberd, "Refined clothespin relocation test and assessment of motion:," *Prosthetics and Orthotics International*, vol. 41, 07 2016.
- [7] C. Gambrell, "Overuse syndrome and the unilateral upper limb amputee: Consequences and prevention." *JPO: Journal of Prosthetics and Orthotics*, vol. 20, pp. 126–132, 07 2008.
- [8] I. Vujaklija and D. Farina, "3d printed upper limb prosthetics," *Expert Review of Medical Devices*, vol. 15, no. 7, pp. 505–512, 2018, pMID: 29949397. [Online]. Available: <https://doi.org/10.1080/17434440.2018.1494568>
- [9] A. Pearson, "10 advantages of 3D printing," <https://3dinsider.com/3d-printing-advantages/>, 01 2018, accessed: 2021-06-24.
- [10] "What are the Advantages and Disadvantages of 3D Printing?" [Online]. Available: <https://www.twi-global.com/technical-knowledge/faqs/what-is-3d-printing/pros-and-cons>
- [11] J. Kate, G. Smit, and P. Breedveld, "3d-printed upper limb prostheses: a review," *Disability and Rehabilitation: Assistive Technology*, vol. 12, pp. 1–15, 02 2017.
- [12] A. Manero, P. Smith, J. Sparkman, M. Dombrowski, D. Courbin, A. Kester, I. Womack, and A. Chi, "Implementation of 3d printing technology in the field of prosthetics: Past, present, and future," *International Journal of Environmental Research and Public Health*, vol. 16, p. 1641, 05 2019.
- [13] O. Uzun, G. Yeginoglu, S. Kalkisim, C. Oksuz, and N. Zihni, "Evaluation of upper extremity anthropometric measurements in terms of sex estimation," vol. 6, p. 42, 01 2018.
- [14] H. Ramachandran, D. Vasudevan, A. Brahma, and S. Pugazhenth, "Estimation of mass moment of inertia of human body, when bending forward, for the design of a self-transfer robotic facility," *Journal of Engineering Science and Technology*, vol. 11, pp. 166–176, 02 2016.
- [15] N. Doriot and X. Wang, "Effects of age and gender on maximum voluntary range of motion of the upper body joints," *Ergonomics*, vol. 49, no. 3, pp. 269–281, 2006, pMID: 16540439. [Online]. Available: <https://doi.org/10.1080/00140130500489873>
- [16] G. Brigstocke, A. Hearnden, C. Holt, and G. Whatling, "The functional range of movement of the human wrist," *Journal of Hand Surgery (European Volume)*, vol. 38, no. 5, pp. 554–556, 2013, pMID: 22918884. [Online]. Available: <https://doi.org/10.1177/1753193412458751>

- [17] Y. Youm, R. Dryer, K. Thambyrajah, A. Flatt, and B. Sprague, "Biomechanical analyses of forearm pronation-supination and elbow flexion-extension," *Journal of Biomechanics*, vol. 12, no. 4, pp. 245–255, 1979. [Online]. Available: <https://www.sciencedirect.com/science/article/pii/0021929079900678>
- [18] J. C. Perry, J. Rosen, and S. Burns, "Upper-limb powered exoskeleton design," *IEEE/ASME Transactions on Mechatronics*, vol. 12, no. 4, pp. 408–417, 2007.
- [19] K. Plewa, J. Potvin, and J. Dickey, "Wrist rotations about one or two axes affect maximum wrist strength," *Applied ergonomics*, vol. 53, 10 2015.
- [20] *Technical Handbook O-rings*, ERIKS, 2021. [Online]. Available: <https://o-ring.info/en/technical-info/>
- [21] "Fused Deposition Modeling," <https://www.materialise.com/en/manufacturing/3d-printing-technology/fused-deposition-modeling>, accessed: 2021-06-24.
- [22] "Multi Jet Fusion," <https://www.materialise.com/en/manufacturing/3d-printing-technology/multi-jet-fusion>, accessed: 2021-06-24.
- [23] "Stereolithography," <https://www.materialise.com/en/manufacturing/3d-printing-technology/stereolithography>, accessed: 2021-06-24.

APPENDIX A: PRINTING DETAILS

TABLE IX
PRINTING PARAMETERS

Print process	Material	Printer	Layer height
SLA	Clear V4 resin	Formlabs Form 3	0.1 mm
FDM	PLA	Ultimaker 3	0.1 mm
MJF	Pa-12	HP Multi Jet Fusion	0.08 mm

FDM properties [21]

- Low-volume production of complex end-use parts
- Prototypes for form, fit and function testing
- Prototypes directly constructed in production materials
- Accuracy is about 0.15% (lower limit on ≈ 0.2 mm)

MJF properties [22]

- Low-volume production of complex end-use parts
- Prototypes for form, fit and function testing
- Prototypes with mechanical properties to rival those of injection-molded parts
- Series of small components as a cost-effective alternative to injection molding
- Accuracy is about 0.3% (lower limit on ≈ 0.3 mm)

SLA properties [23]

- parts with smooth surfaces and fine details
- Low-volume production of complex geometries
- Prototypes for limited functional testing
- Accuracy is about 0.2% (lower limit on ≈ 0.2 mm)

APPENDIX B: COMPRESSION SEALING

To determine the right groove waist GW first the desired groove depth GD must be found. The cord thickness CT of the sealing ring and the clearance gap CG determine this depth by

$$GD = CT - (CG + CT \cdot Comp). \quad (9)$$

Next, the groove waist GW is calculated by subtracting the groove depth GD twice from the piston diameter P , in the equation

$$GW = P - 2 \cdot GD. \quad (10)$$

TABLE X
GROOVE WAIST AND COMPRESSION

Groove waist [mm]	Compression for O-25 [%]	Compression for X and O-262 [%]
7.8	6	4.6
7.9	8	6.5
8.0	10	8.4
8.1	12	10.3
8.2	14	12.2
8.3	16	14.1
8.4	18	16
8.5	20	17.9
8.6	22	19.9

The table of groove dimensions and corresponding compression is shown in Table X. Every 0.1 mm the compression changes 2%, and the accuracy of compression is lower for the X and O-262. So, for the 10% compression a dimension of 8.1 mm comes closest, but is not exactly the desired compression.

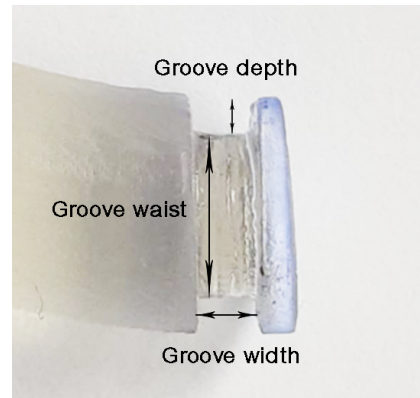


Fig. 31. Groove dimensions with groove depth (GD) groove waist (GW) and groove width

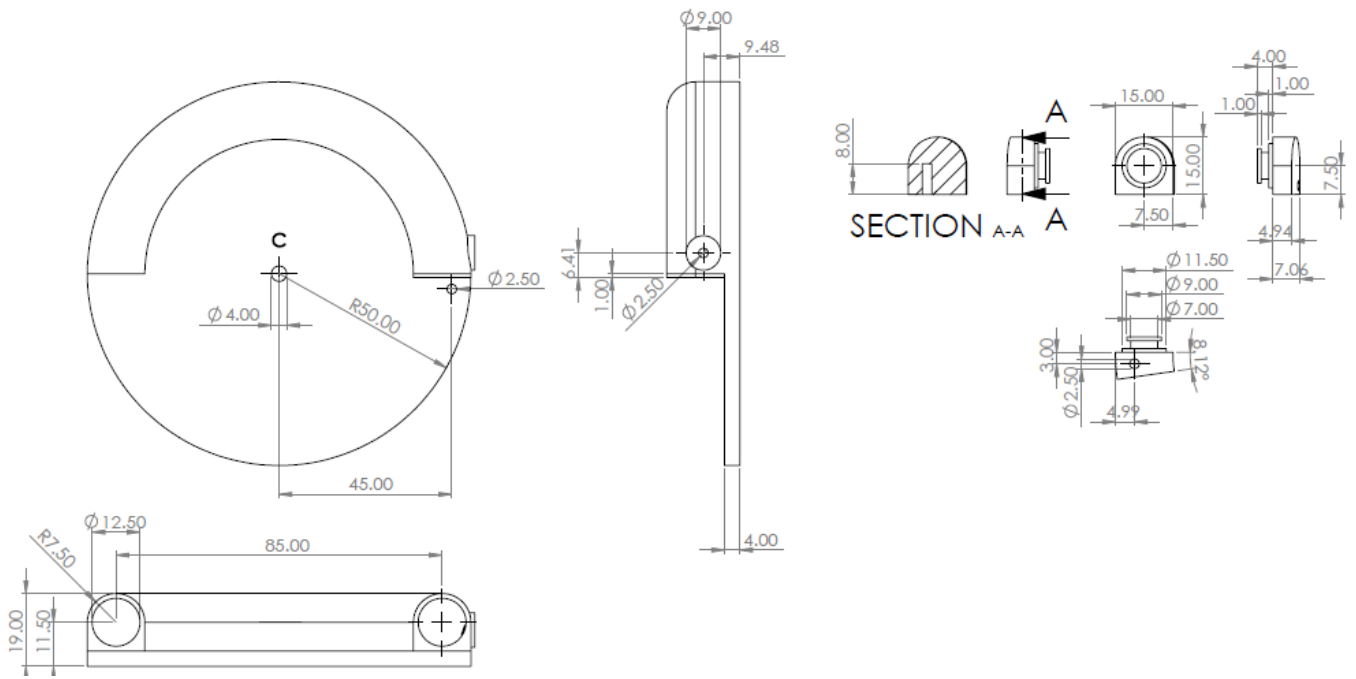


Fig. 36. Dimensional drawing of cylinder C and corresponding plug C

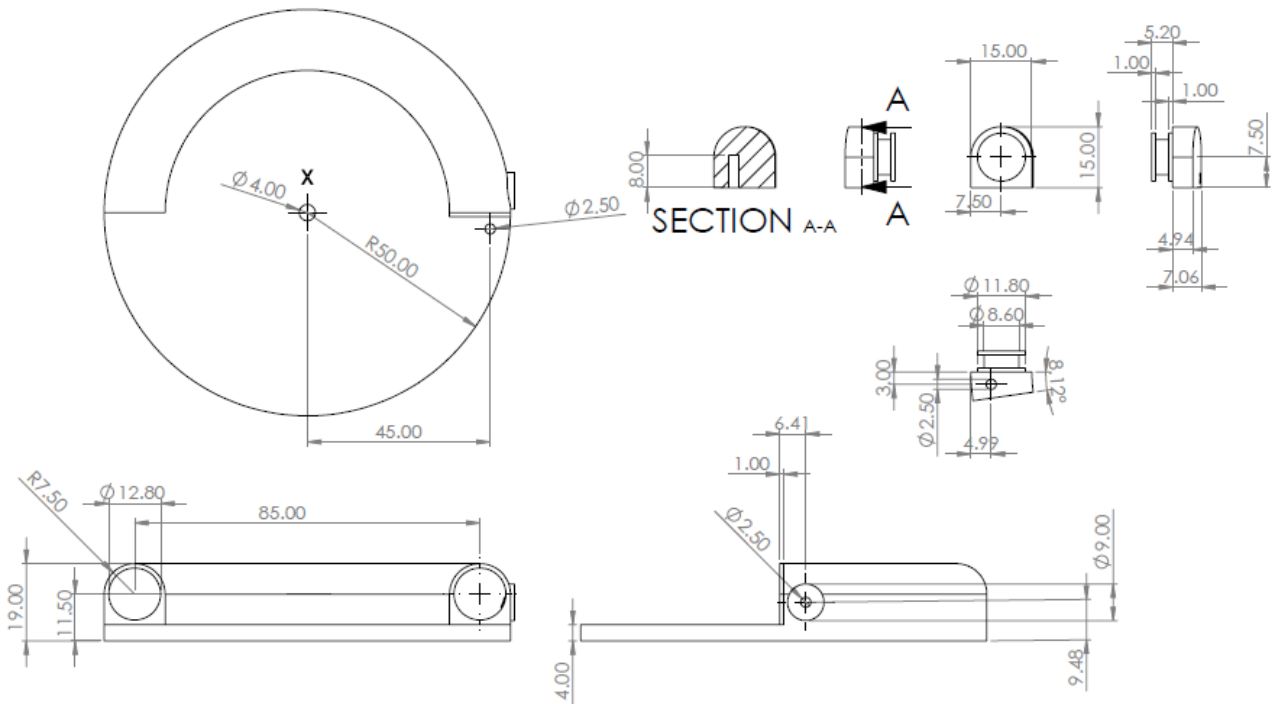


Fig. 37. Dimensional drawing of cylinder X and corresponding plug X

APPENDIX D: OVERVIEW PARTS

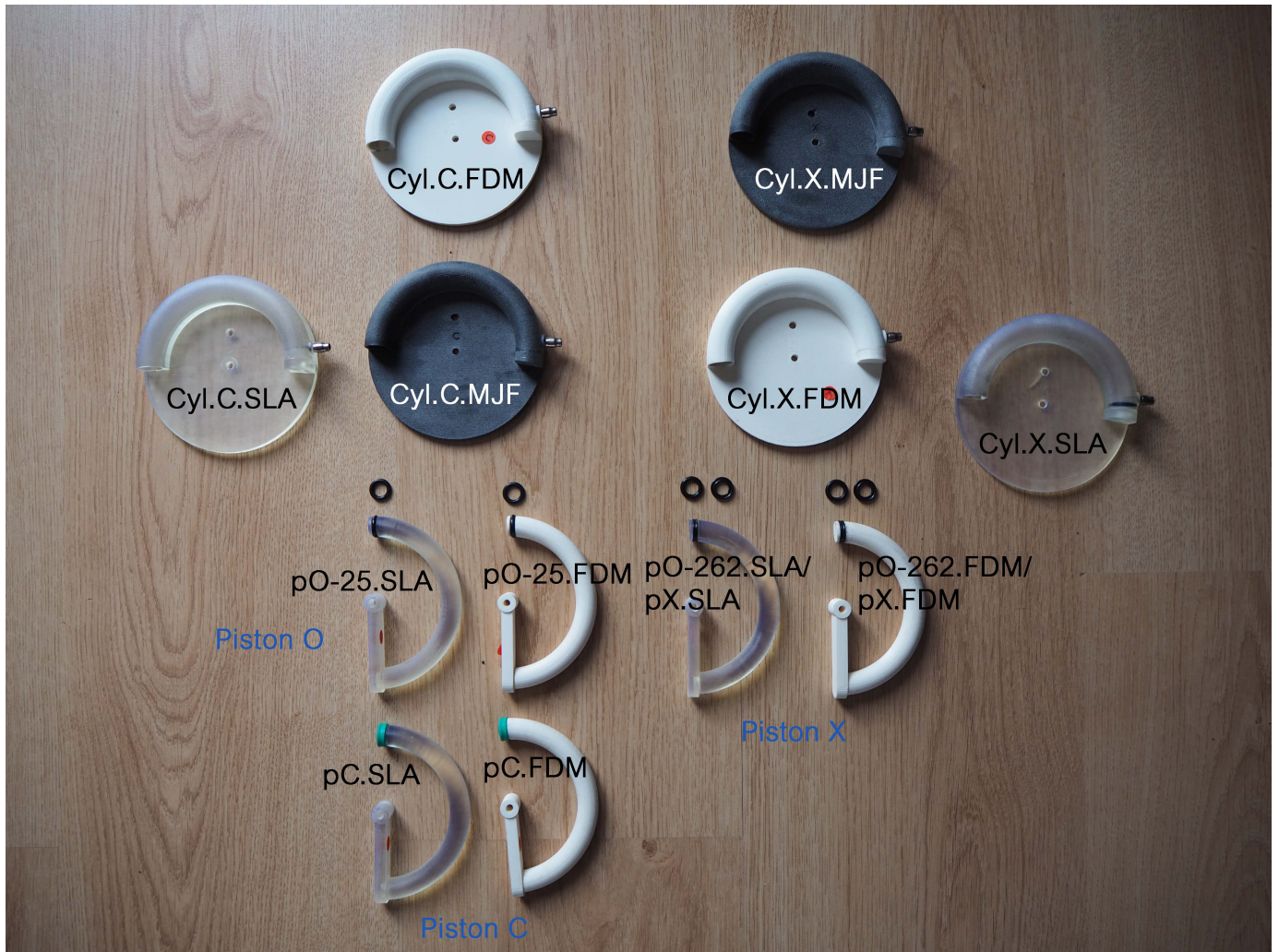


Fig. 38. Overview of all the parts and their names

Current developments in the design of prosthetic wrists: A literature review

Abstract

In the field of upper limb prosthetics research focuses to constantly improve the designs to make them more functional. Still, there is a large rejection rate, so the devices are not yet up to the standard of the user so that they will use them all the time. The focus of research has been greatly on the improvement of hand dexterity and left the field of the wrist prostheses overlooked. Thus, a shift is needed more towards the wrist joints of the upper limb prosthesis.

This literature study investigates the current developments of the prosthetic wrist designs. Firstly, an overview of the currently available wrist designs is made and divided by number of degrees of freedom (DOFs), and DOFs incorporated. Twelve designs are laid out next to each other and their mechanisms are described.

Next, the influence of the different DOFs is explored. Here the pronation/supination and flexion/extension give significant reduction in compensatory movements and improve the performance of activities of daily living (ADLs). A single DOF has some improvement, but combining these two provides even better results, as much as 21 DOFs added in the hand. Not much focus of research has been on the third DOF and its influence.

These results give insight in which designs are out there and the prevalence of DOFs incorporated and mechanisms used. In this overview 2 DOF wrists as most prevalent and the radial/ulnar deviation is the least prevalent DOF. This overview can be used for comparison and support to choose for a certain approach in designing a new wrist prosthesis. The electrically driven prostheses with gears are most common, therefore the hydraulic system should be investigated for new opportunities. Also, the influence of certain DOFs show that the 2 DOF wrists are significantly better than single DOF devices in reducing compensatory movements and completion time. While the influence of the 3rd DOF is unknown.

Keywords: Upper limb prosthesis, wrist design, compensatory movements

I. INTRODUCTION

In the last few decades, research has been performed in the field of upper limb prosthetics to develop and improve the devices. The goal is to give people with an upper limb deficiency the functionality of their missing limb back to engage in their activities of daily living (ADL). The upper limb plays an important role in performing these ADLs. A prosthesis may help these people to live more independently and help them to be able to participate in society. Ultimately, the aim is to give these people the full natural functionality of a healthy human arm. But with more functionality problems arise such as increase of weight and complexity of control. So, a trade-off needs to be found between these properties.

Nowadays, there are still many amputees that will not wear a prosthesis because it does not meet their needs. The reasons that are given by users are weight, discomfort, low functionality, too hard to control, and bulkiness for electric hands. In the adult population, the body-powered hands have the highest rejection rate of 65% compared to electric hands, body-powered hooks and passive hands, which rejection rates vary between 40% and 50%. Overall, about half of the persons with a limb deficiency do not use a prosthesis. (Biddiss et al., 2007) Thus, there is still need for improvement in upper limb prostheses to get devices that people are willing to use, that give more benefits than drawbacks.

The currently commercially available prostheses are mostly a 1 DOF hand with a 1 DOF wrist. This is strongly reduced in DOFs compared to a healthy arm. Combined with the increase of the weight this leads to the problem of compensatory movements. These are the movements made by the user to make up for the lack of DOFs in the hand and wrist. These movements are mostly found in the shoulder, elbow and trunk (Bertels et al., 2009; Carey et al., 2007; Hussaini & Kyberd, 2016) and result in overuse injuries in the long term. (Gambrell, 2008) Reduction of these compensatory movements is an important step in improving the upper limb prosthesis.

In the movements of a healthy person the wrist is an important joint to make natural and smooth movements. A healthy wrist has two DOFs, the first is flexion/extension (FE) and the second is radial/ulnar deviation (RUD). The third DOF considered in design of prosthetic wrists is the pronation/supination (PS) while naturally the pronation/supination is made by the radio-ulnar joint in the forearm. This way the designs of prosthetic wrists can be up to 3 DOF. These wrist movements are important for optimal positioning of the hand when manipulating objects.

Most research has been focused on the increase of the functionality and cosmesis of the hand. By adding DOFs in the hand they provide different gripping patterns and more anthropomorphic looking hands. Also, research has been focused on the development in externally powered prostheses with myo-electric control, but this side of the control will be disregarded in this research. So, while the wrist is an important joint for dexterity the influence of the wrist in prostheses has been overlooked.

To find out what the best direction is to improve upper limb prosthetic design and to address the aforementioned problems, research should be focused on the addition of the wrist and its influence. So, the goal of this study is to find what the current developments are of prosthetic wrist designs and what the influence is of the different DOFs of the wrist on the compensatory movements. This will be done by searching literature on existing wrist designs and their mechanism, to find the possibilities and trends in the design of these devices. Further, in literature will be searched for research that demonstrates the influence on the different DOFs in the wrist and which should at least be included in prosthetic wrist designs.

II. METHOD

This chapter explains how the report is set up. The first step is to determine the scope for this research. The research is about upper limb prosthetics, with the focus on the wrist module. This study investigates the differences between designs and the advantages and disadvantages of the choices made. With this in mind a scope is defined, and search terms are collected for a literature search. There are some terms that are quite obvious to use such as "upper limb", "prosthesis" and "wrist". But there are synonyms and other terms that may or may not be wise to include. But also, some choices made a too long search query that would not fit into the search bar of the search engines. Therefore, some variations were made and compared in the different search engines, namely Scopus and Web of Science, to find out how much results these would give. Results from before the year 2000 were also excluded from the search. The following search queries are used.

Web Of Science: (prosthetic* OR prosthesis) **NEAR/5** (hand OR "upper limb") AND (wrist OR "wrist joint" OR carpal) AND (movement* OR pronation OR supination OR flexion OR extension OR "two degree" OR "2 DOF")

SCOPUS: (prosthetic* OR prosthesis) **W/5** (hand OR "upper limb") AND (wrist OR "wrist joint" OR carpal) AND (movement* OR pronation OR supination OR flexion OR extension OR "two degree" OR "2 DOF")

In this query is chosen to separate the terms 'prosthesis/prosthetic*' and 'hand/upper limb', in contrast to other query options. This gives all the possible variations of these terms together. But to keep the search focused on them together, they still have to be close together in a sentence, hence the NEAR/5 and W/5 in the search query. For this search 452 results were found, with 282 in Scopus and 170 in Web of science.

After scanning through all these papers by reading the abstracts to exclude the irrelevant ones for this research, 71 papers were left that needed to be investigated more thoroughly. In this elimination step the duplicate papers were also removed. And when the full text was unavailable, certain papers could not be used.

Next, these relevant papers have been read entirely to find if they match the scope as expected from reading the abstracts. After this step 22 papers were left, that are going to be used in this report. In this last elimination step, papers were removed that did not fit the scope as suggested by the abstract. Finally, in the most promising papers has been looked at their citations to see if there are other papers that were not found by our own search. This resulted into 4 extra papers, with a total score of 26 papers. This process of elimination is also shown in the flow chart in Appendix A.

III. RESULTS

The two elements of the research goal are treated separately in this section. First the results of the current designs will be reviewed, with focus on the structure and actuation of the designs and the accessory properties. Secondly, the results about the compensatory movements and the influence of the DOFs will be presented.

A. Current design of prosthetic wrist joints

The overview of the designs found is divided based upon the DOFs they provide. An overview of specifications of the wrists is listed in Table 1.

1. Single Degree of Freedom

The first category has only one DOF, this is either pronation/supination or flexion/extension.

The design by Anderson et al. (2012) is a prosthetic device with an electrically powered wrist that provides pronation/supination (Figure 1a). The finger movements are body-powered, controlled with pulleys and wires caused by the shoulder movements. The wrist is actuated by pressure sensors on the toes. These will be activated when an abnormal high force acts on them, causing the wrist to rotate; first one way then the other. The wrist can also rotate towards the closest object due to infrared signal emission from the wrist. The mechanism consists of two disks rotating with respect to each other, activated by a geared motor. Other devices that also use pronation/supination as a single DOF in their wrists are the Otto Bock Wrist rotator, Motion Control electric rotator, MANUS Hand and the Michelangelo hand. (Bajaj et al., 2015)

The design of Schwarm et al. (2019) is a hydrostatic linear actuator with a remote direct-drive manipulator (Figure 1b). It is built up out of two linear actuators, which are floating pistons in between hydraulic fluid and pressurized air, that each control one of the two grip fingers. When the pistons both move away from the gripper, it opens and when they both move towards the gripper, it closes. The wrist flexion/extension is realized when they move in opposite direction, one extends and one contracts, this way the grip fingers can move together upward and downward. According to Schwarm et al. (2019) this system has low friction with high torque density. In contrast to traditional hydraulic or pneumatic systems this also give the possibility for 'backdrivability' and passive tuneable compliance.

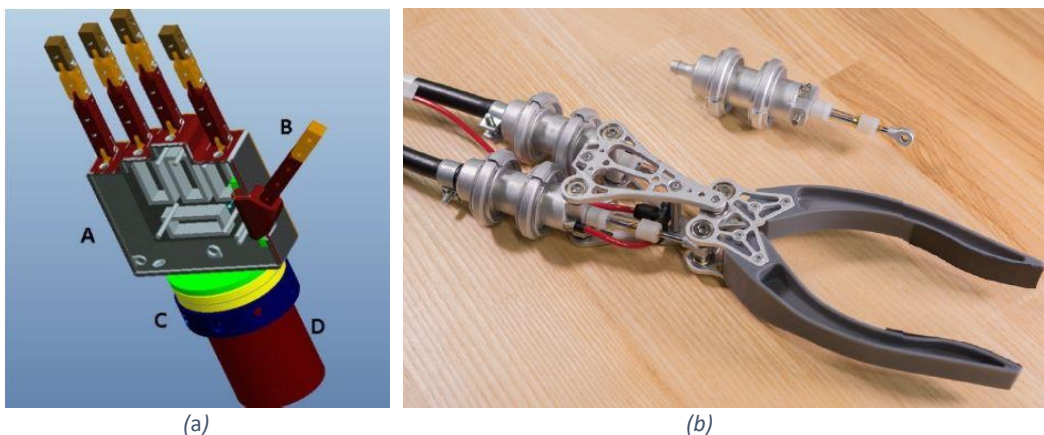


Figure 1: Single DOF devices, design by Anderson (a) and the Piston gripper, design by Schwarm (b).

2. Two Degrees of Freedom

Two degrees of freedom can be either a combination of the aforementioned pronation/supination and flexion/extension, or a combination of flexion/extension and

radial/ulnar deviation. First the designs of the pronation/supination and flexion/extension combination are mentioned and after that the designs with flexion/extension and radial/ulnar deviation combinations.

a. Pronation/supination and flexion/extension

Chu et al. (2011) shows a design of a myoelectric underactuated hand, with in total 18 DOF initiated by 4 actuators (Figure 2a). There are two actuators for the hand movements and two for the wrist. The actuators for the wrist are DC motors and placed in the forearm. The mechanism is built up with three bevel gears and two worm gear sets. The proximal joint is able to perform flexion/extension, and the distal one is for pronation/supination. So, when the hand is rotated 90 degrees this same movement that causes the flexion/extension becomes the radial/ulnar deviation.

Kyberd, Lemaire et al. (2011) describes a design of a 2 DOF wrist prosthesis that makes use of the mechanical differential. With this differential activation of the two motors becomes one motion, but with twice as much torque possible to be applied. The combined motion that results is dependent on the relative speed of the two motors. The same direction of the motors results in one DOF and the opposite direction in the other DOF. The pronation/supination movement is proximal to the flexion/extension movement. In this design none of the elements are placed in the forearm, to broaden the target audience. With the elements all placed in the hand, the design is available for people with long residual limbs. The two motors that actuate the wrist movement are placed parallel in the hand palm (Figure 2b).

The DEKA arm that is elaborated in the study of Resnik et al. (2013) is an externally powered upper limb prosthesis (Figure 2c), with different versions based on the level of amputation: transradial, transhumeral, and shoulder level. In their study two versions are discussed: the Gen 2 and Gen 3. They have the same basics, but Gen 3 has some different elements and is an optimization of Gen 2. This arm is controlled by movement of the foot, where force sensitive resistors (FSR) or inertial measurement units (IMU) are placed, with a battery and arm input control unit (ACI) around the ankle. This is connected to the master control module (MCM) and battery in a belt around the waist, from where the arm is controlled. This prosthesis has pre-programmed grip patterns and wrist movements. Here the wrist movements are coupled, the wrist flexion together with the ulnar deviation and the wrist extension with the radial deviation. A safety button is added in the Gen 3, for when the system does not respond, this way the hand can be opened again.

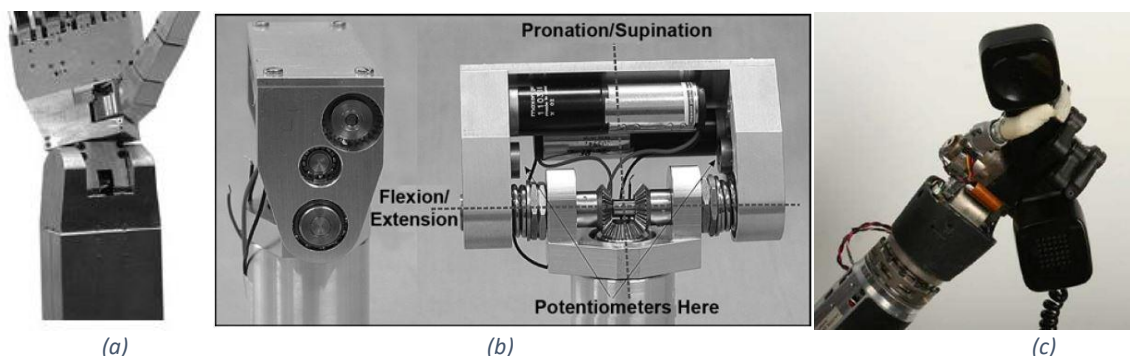


Figure 2: 2 DOF wrists with PS and FE, underactuated design by Chu et al. (2011) (a), The Differential, design by Kyberd, Lemaire et al. (2011) (b), and the DEKA Arm, design by Resnik et al. (2013) (c).

The HyPro hybrid powered prosthesis (Figure 3a), a design by Semasinghe et al. (2017) has a fully electric powered wrist. The body-powered part is focused on the use of the fingers. The wrist joint in this design is built up in two units with each its own servomotor. The proximal unit is attached to the forearm and provides the pronation/supination motion, it

causes the distal unit to rotate with respect to the proximal one. The distal unit causes the flexion/extension movement.

The Octa Hand (Figure 3b) is a design by Abarca et al. (2019) where the wrist is an active member of an active hand prosthesis. Pronation/supination is induced by a helical gear that rotates the shaft of the wrist module, on the proximal side, around the centre connected to the forearm. And the flexion/extension movement is induced by a worm gear that causes the tilt on the distal side of the shaft, only causes the hand to tilt, the wrist itself stays in place. This system is active, therefore there is also a DC motor placed inside the wrist module this is actuated by a microcontroller and LiPo battery. And because the device is position controlled there are two position sensors placed in the wrist, one for each DOF.

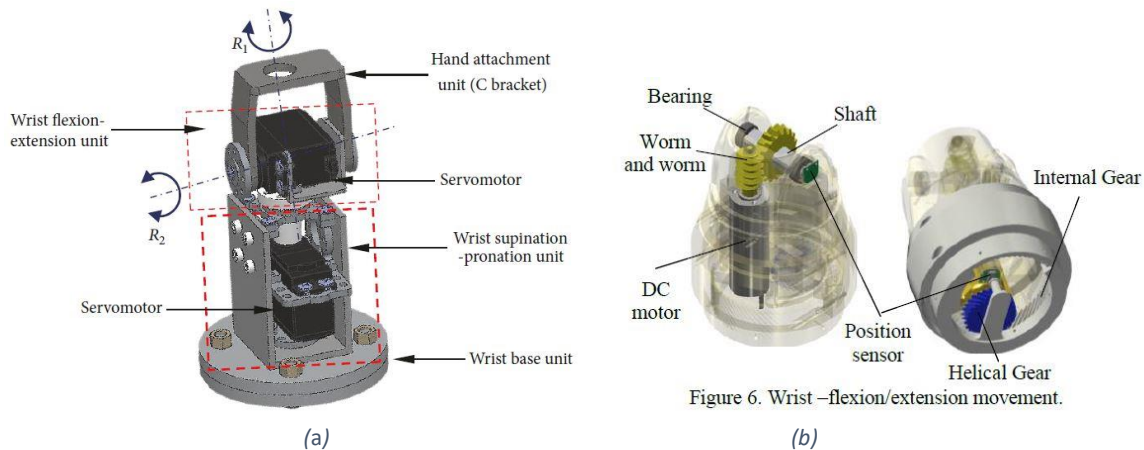


Figure 3: 2 DOF wrists with PS and FE, design by Semasinghe et al. (2017): HyPro (a) and design by Abarca et al. (2019): Octa Hand (b)

b. Flexion/extension and radial/ulnar deviation

The ARTS wrist by Tropea et al. (2008) has a resemblance to a spring rider (Figure 4a). This design consists of three parallel disks, where the two on the top are held apart by a thrust spring. And by means of three cables that are connected to the top disk, and run through the middle disk, the top disk can be tilted. This way the system provides the movements flexion/extension and radial/ulnar deviation. The cables are actuated by three motors that are placed between the two lower disks.

Bandara et al. (2014) propose a design of a multi-DOF anthropomorphic prosthetic arm (Figure 4b). This design is actuated by parallel prismatic manipulators, making it look like the anatomy of the lower arm, with the two linear actuators representing the radius and the ulna. They are connected to two plates, the distal one is the wrist plate that can be moved with respect to the actuators. The movements are made by retracting and extending the actuators. When one actuator extends and the other retracts the wrist plates tilt sideways causing radial/ulnar deviation. And when the actuators make similar movements, they cause the flexion/extension motion, by tilting the wrist plate upward and downward. When both actuators extend, they cause extension of the wrist joint and when both retract, they cause flexion.

The passive wrist with switchable stiffness by Montagnani et al. (2017) is a hydraulic operated wrist joint based on the Delft Cylinder hand. The joint itself is a standard ball joint, with a ball and a socket. Around this joint there are four hydraulic cylinders, at an equal distance from each other, an intersection is shown in Figure 4c. The opposite cylinders are connected, and in between in these two there is a valve that can open allowing the fluid to

flow resulting a compliant wrist, enabled by springs that are attached to the wrist base. And when the valve is closed, the fluid cannot flow resulting in a stiff wrist. The opposite cylinders are connected separately enabling the flexion/extension and radial/ulnar deviation happen separately. This system is a passive one, causing the user to use his body to manipulate the joint, this can be done by pushing it against a stiff surface. They want the prosthesis to be compliant when reaching and stiff when grasping and manipulating objects.

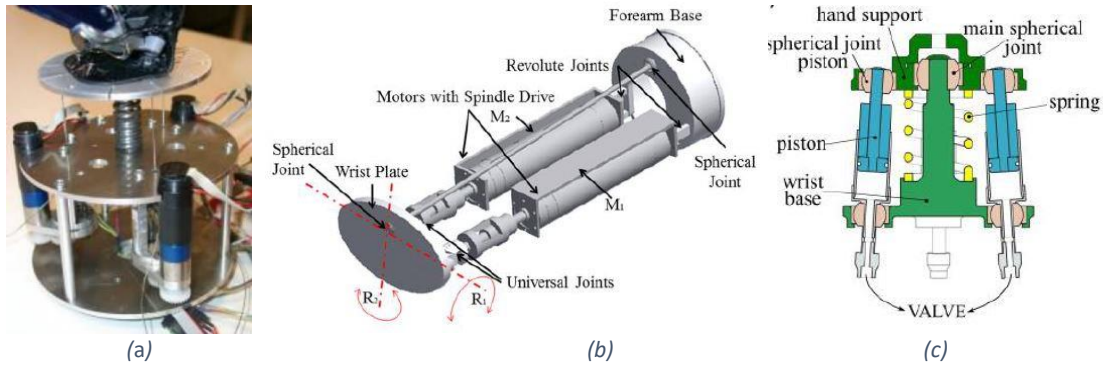


Figure 4: 2 DOF designs combining FE and RUD, ARTS wrist by Tropea et al. (2008) (a), Anthropomorphic design by Bandara et al. (2014) (b), and passive wrist design by Montagnani et al. (2017) (c)

3. Three Degrees of Freedom

The design of Jarc et al. (2006) is a prosthetic limb where all the joints include a control moment gyroscope (CMG), with a rotating disk inside that causes the movements in different directions (Figure 5a). This causes the joints to be able to have 3 DOF. Due to this CMG the wrist has a larger size than other prosthetic arms, the wrist has a diameter of 11.45 cm. Besides the high number of DOF it also has a reduced power consumption with the CMG.

The Gas actuated design (Figure 5b) proposed by Fite et al. (2007) has a 3 DOF, wrist and is based on anthropomorphic design. The pronation/supination motion is generated by two cylinders in the same axis that can rotate with respect to each other. The distal cylinder is smaller and placed partially in the proximal cylinder and are connected together by a leadscrew path on the cylinders. The other two DOFs are actuated by two cylinders that are placed parallel to the distal cylinder, one for flexion/extension and one for radial/ulnar deviation. They each have a transmission from the movement of the cylinder becoming longer and shorter to the desired movement. The flexion/extension transmission is by means of a pinned joint and the radial/ulnar deviation cylinder has a spherical joint at the end.

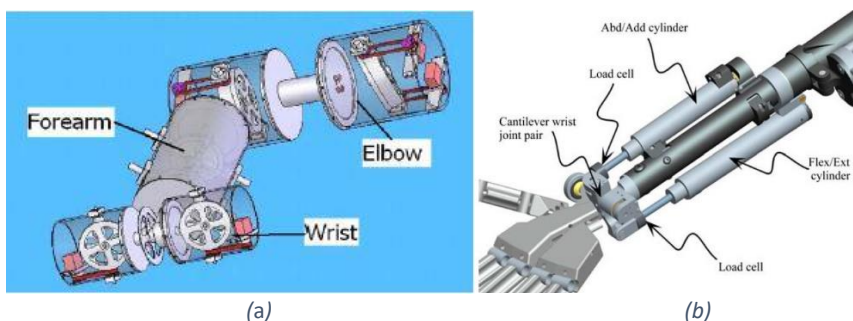
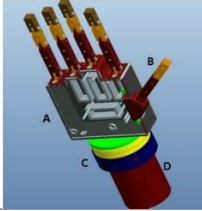
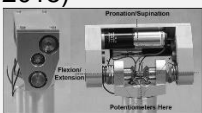
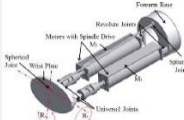
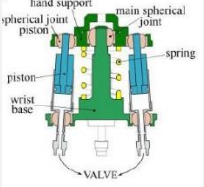
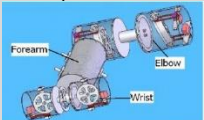
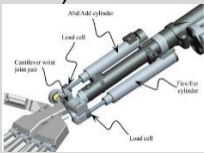


Figure 5: 3 DOF wrists, a CMG controlled design by Jarc et al. (2006) (a) and a Gas actuated design by Fite et al. (2007) (b)

Table 1: Comparison specifications of current design

	# D O F	Degrees	Active/ Passive	Mechanis m	Torque [Nm]	Joint Speed [deg/s]	Own weight [kg]	Weight carried [kg]
Body-powered autorotation (Anderson et al., 2012) 	1	PS: 360°	Active	Gears, disks	5.65	3.6	- Est. 0.2	-
Piston gripper (Schwarm et al., 2019) 	1	FE: 120°	Active	Hydraulic	-	-	- Est. 0.1	-
Underactuated hand (Chu et al., 2011) 	2	PS: 360° FE: 180°	Active	Bevel and worm gears	-	-	0.2	-
DEKA Arm (Resnik et al., 2013) 	2	PS: - FE: -	Active	Gears, disks	-	-	1.13 (Gen2) 1.27 (Gen3) (hand + forearm)	-
The differential (Kyberd et al., 2015) 	2	PS: - FE: -	Active	Gears	0.073 (for 500mA, 7V)	250 (peak) 175 (const ant)	- est. 0.2	-
HyPro: hybrid (Semansinghe et al., 2017) 	2	PS: 180 (-90; 90) FE: 145 (-75; 70)	Active	Gears	-	-	- est. 0.2	-

	# D O F	Degrees	Active/ Passive	Mechanis m	Torque [Nm]	Joint Speed [deg/s]	Own weight [kg]	Weight carried [kg]
Octa Hand (Abarca et al., 2019) 	2	PS:180° (-90; 90) FE: 70°	Active	Helical gear (PS) Worm gear (FE)	1.43	±200	0.640-0.760 (wrist +forearm)	0.5 hand + 0.5 weight
ARTS wrist (Tropea et al., 2008) 	2	FE: 60° (-25 35) RU: 55° (-25; 30)	Active	Cables	-	-	- Est. 0.3	0.5 hand + 4 added weight
Anthropomorphic arm (Bandara et al., 2014) 	2	FE: 88° (-43; 45) RU: 52° (-21; 31)	Active	Linear actuators, gears	1.2	FE: 41/17 RU: 14	0.5	-
Passive wrist (Montagnani et al., 2017) 	2	FE: 70° (-35; 35) RU: 70° (-35; 35)	Passive	Hydraulic	reaction torque: 0.8	-	0.13	4.9 (stiff) 0.9 (compl.)
CMG-driven (Jarc et al., 2006) 	3	PS: - FE: - RU: -	Active	Control moment gyroscope (CMG)	6.56	Up to 78000	- Est. 0.2	2.7
Gas-Actuated (Fite et al., 2007) 	3	PS:95 ° FE:105° RU: 40°	Active	Pneumatic	PS:4.2 FE: 4.5 RU: 4.5	-	2 (whole arm)	-

B. The positive influence of a wrist joint in a prosthesis

Earlier studies demonstrated that wrist movement in upper limb prostheses was desired by prosthetics users (Biddiss et al., 2007). Besides the basic priorities of weight, costs and comfort, where still improvement is needed, the increase of functionality including wrist control is an important priority for the users (Biddiss et al., 2007). In another study by Pylatiuk et al. (2008) 70% of the prosthetics users found the flexion/extension useful.

When there is no wrist joint in the prosthetic arm, the user needs to compensate for the lack of DOFs. Different studies have researched what the compensatory movements are using current prosthetic devices and investigated whether these movements are reduced by adding certain DOFs in the wrist. In the design of upper limb prosthetics, the most applied DOF in the wrist is pronation/supination.

The absence of DOFs in the wrist causes the user to make different movement while performing an activity when compared to a healthy person. Carey et al. (2007) found that there was a significant difference in shoulder and elbow movements when comparing these two conditions. When the DOFs of the wrist are inhibited, the elbow and shoulder have an increased ROM when performing the same task. When performing a bimanual task, such as lifting a box, the healthy side compensates for the lack of DOFs in the prosthetic side. The shoulder and elbow flex more, resulting in asymmetry in the movement. Additionally, they added mass to mimic the increased mass of a prosthetic device, which resulted in increase of compensatory movements.

In performing the Clothespin Relocation Task with a 1 DOF hand prosthesis the user makes more trunk movements than a healthy person does (Hussaini & Kyberd, 2016). The highest ROM was when the clothespin needed to be placed on the highest point. Besides the presence of compensatory movements, the duration to perform the test with the prosthesis increases. Especially in the downward movement where the clothespins need to be placed on a horizontal rod. Here the completion time and the ROM is a measure for qualitative movement, where a lower value means a better performance. The trunk movements are to compensate for the lack of DOF in the forearm which is needed to rotate the hand to move the clothespins from a horizontal rod to a vertical rod and the other way around. This corresponds with the results found by Kato et al. (2018) where the focus was on the torque that was applied in the shoulder joint. They found that there was more flexion by the trunk than movement in the shoulder joint as compensatory movements.

Adding a wrist rotator to a prosthesis gives better performance in carrying out tasks, and closer to anatomical movement (Lura et al., 2008). However, for a large number of joints there are no significant differences. Especially in the task where the participant has to open a door, the trajectory of certain joints is similar between a prosthesis with and without a wrist and deviate from the optimal movement. When it comes to compensatory movements there is a collaboration between joints, over which the movement is distributed, so it is hard to objectify the movements for different body parts (Montagnani et al., 2015a).

There is also a synergy between the position of the wrist and the deviation of the upper arm (Montagnani et al., 2015a). In this study the person has only 1 DOF in the wrist, namely pronation/supination. With this one DOF device they compared the ROM of the compensatory movements in certain tasks, with the wrist in either pronated, supinated or neutral position. When fully supinating the forearm, the humeral deviations are small. The arm stays adjacent to the body. When the forearm is in neutral position there are small movements in the upper arm, but larger than in supinated position. And during activities with the forearm fully pronated the humeral movements have the highest ROM.

In developing upper limb prosthetics, the focus has been more on increasing the hand dexterity than the wrist. Yet, Montagnani et al. (2015b) found that adding a second DOF to the wrist has an equal performance in performing ADLs as adding 21 DOF in the hand. This shows the importance of the second DOF of the wrist, adding flexion/extension to the pronation/supination movement. Just having 1 DOF hand and 1DOF wrist combined, the most available used, gives significant compensatory movements that are reduced when adding more DOFs.

In addition, the flexion/extension movement of the wrist has positive influence on the quality of movements (Deijs et al., 2016). In this study, using the flexible wrists gave more natural movement patterns, less awkward positions, less burden on the shoulder, and increased dexterity. Plus, the participants of this study were more satisfied in performing the tasks with wrist flexion.

Kyberd (2011) also researched the influence of wrist flexion on the performance of certain tasks. They found that adding flexion in the wrist resulted into overall better performance, especially in lateral grip and tips grip. Also, they compared a fixed flexion wrist with a compliant wrist. For the fixed flexion the power grip also performed significantly better than without flexion. And the compliant wrist had a better performance for the extension grip.

The degree of flexion has influence on the reduction of compensatory movements. Bertels et al. (2009) investigated the difference between a flexed hand of 20° and 40°, compared to no flexion. The motions that were reduced are the anteversion of the arm and the humeral rotation, that compensate for the lack of flexion. The 20° angle gives no significant results on the anteversion while 40° comes halfway towards the trajectory of a natural movement. Also, the shoulder elevation, which is linked to trunk flexion, is significantly reduced with the 40° angle. Eighty percent of the participants felt that flexion positively influenced the motion. Half of the 30 performed tasks were preferred with the 40° angle. Nine other motions were preferred with the 20° angle, and the for the rest of the motions there were no preferences.

A recent study by Davidson et al. (2018) found that the Dart Thrower's Motion (DTM) is preferred by prosthetics users over the pronation/supination movement. This DTM is a combination of ulnar deviation with flexion in an angle of 20°- 40° with respect to the sagittal plane. Here the activities that needed to be performed were ADL's where the DTM is used normally, and they cannot be easily performed with compensatory movements. The preference of DTM over pronation/supination is because the last one can be overcome by abduction of the shoulder.

IV. DISCUSSION

To find the best direction for design of a prosthetic wrist, the benefits of the different DOFs are investigated and the trends in existing wrist designs are reviewed. The results found in this paper are discussed below.

Firstly, from the twelve found prosthetic wrist designs most include the pronation/supination and flexion/extension movements. In the 2 DOF category designs that combine pronation/supination and flexion/extension are more common than the flexion/extension with radial/ulnar deviation combined. The radial/ulnar deviation is not even found as a single DOF device. This is a logical choice because in a healthy wrist radial/ulnar deviation is the DOF with the smallest ROM. Research is therefore more focused on the other two DOFs, because it is expected that these will have the largest positive influence on the functionality when added. This is also found in the different studies that investigate the influence of the DOFs pronation/supination and flexion/extension. These DOFs are beneficial for the performance of activities (Bertels et al., 2009; Hussaini & Kyberd, 2016; Kyberd, 2011; Lura et al., 2008; Montagnani et al., 2015a; Montagnani et al., 2015b). However, no studies are found about the influence of radial/ulnar deviation.

Overall, adding a certain DOF, either pronation/supination or flexion/extension, showed improvement in reducing compensatory movements and task completion time. Even when the test did not find significant difference in certain movements, the positive influence in movement was noticed, either by observation of the test or experienced by the participants (Lura et al., 2008). This lack of significant results could be due to the fact that the compensatory movements are performed differently by individuals. Or the compensatory movements could be distributed over certain joints, so it is not significantly shown in the body part where it was measured. So, subjectively the improvement of compensatory movement is noticed more often than objective positive results.

Montagnani et al. (2015b) even found that the second DOF, adding the flexion/extension to pronation/supination, has as much increase in performance as a 21 DOFs of the hand. This supports the importance of these DOFs of the wrist, and its influence on the dexterity and functionality. These two DOFs have shown significant benefits while little is found about the benefits of adding the radial/ulnar deviation as extra DOF.

While 2 DOF is found to have the most benefit, they are also the most prevalent. The ultimate goal is to make a prosthesis that has the full functionality of a healthy arm, with a 3 DOF wrist. But with increase of the number of DOFs problems with increase in dimension, weight and control complexity occur. So, more research on the influence of the addition of the 3rd DOF is necessary to find the optimum between the functionality and the control complexity. Where high functionality and low control complexity is desired.

Although the size and weight are two important design considerations for upper limb prosthetics and also cause of rejection (Biddiss et al., 2007) there are no guidelines for these properties. The 2 DOF wrists with the pronation/supination and flexion/extension combination are built mostly in sequential architecture, where one joint is placed more distal than the other. This sequential design results in longer wrist units, and higher total length of the prosthesis, when not compensated with a shorter forearm. This length should be limited because the length of the prosthetic arm should be as close as possible to the length of the healthy arm of the subject. Reducing the forearm limits the option for people with longer residual limbs to use prosthesis. There also lies a problem for active hands, because the forearm is often used to place the actuators and other elements. Likewise, the anthropomorphic designs by Bandara et al. (2014) and Fite et al. (2007) are not suitable for long residual limbs, due to the size of the prismatic joints involved. Meanwhile, the

flexion/extension and radial/ulnar deviation combination has the ability to be placed parallel, e.g. by means of a ball and socket joint. That would be beneficial for limiting the size of the wrist. The only device found with this spherical joint is a passive hydraulic wrist. The possibility for parallel placements of the two most used DOFs can help limit the length of the wrist unit.

Further, the most prevalent wrist designs found are active and electrically driven devices with gear mechanisms, that due to all the batteries and actuators involved, are the heaviest type. Despite the high functionality of these devices the control complexity and increase of weight cause problems. More weight results in more strain on the arm and results into more compensatory movements as found by Carey et al. (2007). To assess the problems of compensatory movements with this property, more focus should be on lightweight alternatives or reduction in electric elements. This can be underactuated design or different actuation such as hydraulics or pneumatics.

Next, the compensatory movements are measured by some studies is the shoulder abduction and anteversion (Bertels et al., 2009), other studies show that there is more movement in the trunk (Hussaini & Kyberd, 2016). They do not contradict each other; they show the different effect of the same compensation. This has to do with the certain tasks that are performed. Which was found by Montagnani (2015a) where the position of the hand, pronation or supination, influences the amount of compensatory movements. This was not found for flexion, however. The trunk motion is noticed in the clothespin relocation task, where the lack of rotation was assessed. Shoulder elevation is expected because the task requires a pronated hand. However, this is a precision task, and the humerus is kept close to the side to get support by the torso when picking and placing the objects. With this support, the hand is more stable and makes it easier to perform the task.

Lastly, Davidson et al. (2018) found that the Dart Thrower's Motion preferred over the pronation/supination, because they could overcome the latter easily with compensatory movements in the shoulder and the trunk. Yet, this research shows bias towards the DTM because the performed activities in their test required only the DTM. Plus, the activities where hard to compensate for with other movements, which makes these tasks look harder to complete. However, because users are interested in the application of this movement and the lack of research done into the influence of the radial/ulnar deviation, this is a promising direction for further research. With the information about the benefits of this 3rd DOF, it can be compared to the other DOFs that reduce the compensatory movements and a better decision can be made about which DOFs to include. Ultimately the radial/ulnar deviation is added as the third DOF to come closer to the functionality and dexterity of a healthy hand. With this information also a better trade-off can be made between increasing the functionality and the increase of dimensions and control complexity.

V. CONCLUSION

To conclude, for the design of a new prosthetic wrist that addresses the problems of rejection rates and compensatory movements the focus should be on a light weight, small and functional design with low control complexity. Within these properties trade-offs needs to be made to find the optimal achievable design.

The current wrist designs are mostly active, electrically driven, 2 DOF devices that include pronation/supination, and built in a sequential order. No guidelines or restrictions are found for the properties of size and weight, while these are important factors of rejection.

To minimize the length of the device, there should be looked into the possibility of parallel placement of the rotation axes of the different DOF joints. The anthropomorphic designs are less suitable, due to the size of their prismatic joints in the lower arm. Because that excludes the use for people with longer residual limbs.

Low weight is mostly an issue for active prostheses, because the presence of batteries and actuators. To minimize the weight these elements should be minimized in size and number, with underactuated design. With the electrically driven prostheses as most prevalent, opportunities may be found in other directions, therefore the hydraulically driven prostheses should be investigated.

Finally, for good functionality the joint should have at least 2 DOFs, namely the pronation/supination and flexion/extension. Since the importance of adding a single DOF of the wrist is found to be more beneficial than the increase in dexterity of the hand. The influence of the third DOF of the wrist is unknown. So, the radial/ulnar deviation should be researched more to see where the benefits of this DOF lie and if they are significant to incorporate in wrist design as the 3rd DOF and weighs off to the increase of complexity.

REFERENCES

- Abarca, V., Flores, K. & Elias, D. (2019). The Octa Hand: An Affordable Multi-Grasping 3D-Printed Robotic Prosthesis for Transradial Amputees. 92-97. 10.1109/ICCAR.2019.8813417.
- Anderson, E., Moloughney, J., Ozerinsky, K. & Saleh, R. (2012). Body powered anthropomorphic prosthetic hand with force feedback and auto-rotation regimes. 33-34. 10.1109/NEBC.2012.6206948.
- Bajaj, N., Spiers, A. & Dollar, A.. (2015). State of the Art in Prosthetic Wrists: Commercial and Research Devices. 2015. 10.1109/ICORR.2015.7281221.
- Bandara, S., Gopura, R., Hemapala, K. T. M. U. & Kiguchi, K. (2014). A multi-DoF Anthropomorphic Transradial Prosthetic Arm. Proceedings of the *IEEE RAS and EMBS International Conference on Biomedical Robotics and Biomechanics*. 10.1109/BIOROB.2014.6913917.
- Bertels, T., Schmalz, T. & Ludwigs, E. (2009). Objectifying the Functional Advantages of Prosthetic Wrist Flexion. *JPO: Journal of Prosthetics and Orthotics*. 21. 74-78. 10.1097/JPO.0b013e3181a10f46.
- Biddiss, E., Beaton, D. & Chau, T. (2007). Consumer design priorities for upper limb prosthetics. *Disability and Rehabilitation. Assistive technology*. 2. 346-57. 10.1080/17483100701714733.
- Carey, S., Highsmith, M. & Dubey, R. (2007). Range of Motion of Upper Limb Joint Angles During Two Tasks for Transradial Prosthetic Design. 10.1115/DETC2007-35349.
- Chu, J. U., Jeong, D. H., Youn, I., Choi, K. & Lee, Y. J. (2011). Myoelectric Hand Prosthesis with Novel Adaptive Grasping and Self-locking. *International Journal of Precision Engineering and Manufacturing*. 12. 10.1007/s12541-011-0146-0.
- Davidson, M., Bodine, C. & Weir, R. (2018). User surveys support designing a prosthetic wrist that incorporates the Dart Thrower's Motion. *Disability and Rehabilitation: Assistive Technology*. 14. 1-4. 10.1080/17483107.2018.1447607.
- Deijs, M. & Bongers, R., Leusen, N. & Sluis, C. (2016). Flexible and static wrist units in upper limb prosthesis users: Functionality scores, user satisfaction and compensatory movements. *Journal of NeuroEngineering and Rehabilitation*. 13.
- Fite, K., Withrow, T., Wait, K. & Goldfarb, M. (2007). A Gas-Actuated Anthropomorphic Transhumeral Prosthesis. 3748 - 3754. 10.1109/ROBOT.2007.364053.10.1186/s12984-016-0130-0.
- Gambrell, C. (2008). Overuse Syndrome and the Unilateral Upper Limb Amputee: Consequences and Prevention. *JPO: Journal of Prosthetics and Orthotics*. 20. 126-132. 10.1097/JPO.0b013e31817ecb16.
- Hussaini, A. & Kyberd, P. (2016). Refined clothespin relocation test and assessment of motion:. *Prosthetics and Orthotics International*. 41. 10.1177/0309364616660250.
- Jarc, A., Kimes, A.B., Pearson, M.E. & Peck, M.A.. (2006). The Design and Control of a Low-Power, Upper-Limb Prosthesis. 165 - 166. 10.1109/NEBC.2006.1629804.
- Kato, Akira & Nagumo, Haruno & Tamon, Miyake & Fujie, Masakatsu & Sugano, Shigeki. (2018). Evaluation of Compensatory Movement by Shoulder Joint Torque during Gain Adjustment of a Powered Prosthetic Wrist Joint. *Conference proceedings: ... Annual International Conference of the IEEE Engineering in Medicine and Biology Society. IEEE Engineering in Medicine and Biology Society. Conference*. 2018. 1891-1894. 10.1109/EMBC.2018.8512594.
- Kyberd, P. (2011). The influence of passive wrist joints on the functionality of prosthetic hands. *Prosthetics and orthotics international*. 36. 33-8. 10.1177/0309364611426905.
- Kyberd, P., Lemaire, E., Scheme, E., MacPhail, C., Goudreau, L., Bush, G. & Brookshaw, M. (2011). Two-degree-of-freedom powered prosthetic wrist. *Journal of rehabilitation research and development*. 48. 609-17. 10.1682/JRRD.2010.07.0137.
- Lura, D., Dubey, R., Carey, S. & Highsmith, M. (2008). Simulated Compensatory Motion of Transradial Prostheses. 10.1115/IMECE2008-67842.
- Montagnani, F., Controzzi, M. & Cipriani, C. (2015). Exploiting Arm Posture Synergies in Activities of Daily Living to Control the Wrist Rotation in Upper Limb Prostheses: a Feasibility Study. 10.1109/EMBC.2015.7318892.
- Montagnani, F., Controzzi, M. & Cipriani, C. (2015). Is it Finger or Wrist Dexterity That is Missing in Current Hand Prostheses?. *IEEE Transactions on Neural Systems and Rehabilitation Engineering*. 23. 10.1109/TNSRE.2015.2398112.
- Montagnani, F., Smit, G., Controzzi, M., Cipriani, C. & Plettenburg, D. (2017). A passive wrist with switchable stiffness for a body-powered hydraulically actuated hand prosthesis. *IEEE ... International Conference on Rehabilitation Robotics : [proceedings]*. 2017. 10.1109/ICORR.2017.8009412.
- Pylatiuk, C., Schulz, S. & Döderlein, L. (2008). Results of an Internet survey of myoelectric prosthetic hand users. *Prosthetics and orthotics international*. 31. 362-70. 10.1080/03093640601061265.
- Resnik, L. Klinger, S. & Etter, K. (2013). The DEKA Arm: Its features, functionality, and evolution during the Veterans Affairs Study to optimize the DEKA Arm. *Prosthetics and orthotics international*. 38. 10.1177/0309364613506913.

Schwarm, E., Gravesmill, K. & Whitney, J. (2019). A Floating-Piston Hydrostatic Linear Actuator and Remote-Direct-Drive 2-DOF Gripper. 7562-7568. 10.1109/ICRA.2019.8794378.

Semasinghe, C., Ranaweera, R. K. P. S., Prasanna, B., Kandamby, H., Madusanka, K. & Gopura, R. (2017). HyPro : A multi-DoF Hybrid Powered Transradial Robotic Prosthesis. *Journal of Robotics*. 2018. 10.1155/2018/8491073.

Tropea, P., Stellin, G., Carrozza, M. C. & Dario, P. (2008). Development of an innovative and compliant robotic wrist. 10.1109/BIOROB.2008.4762834.

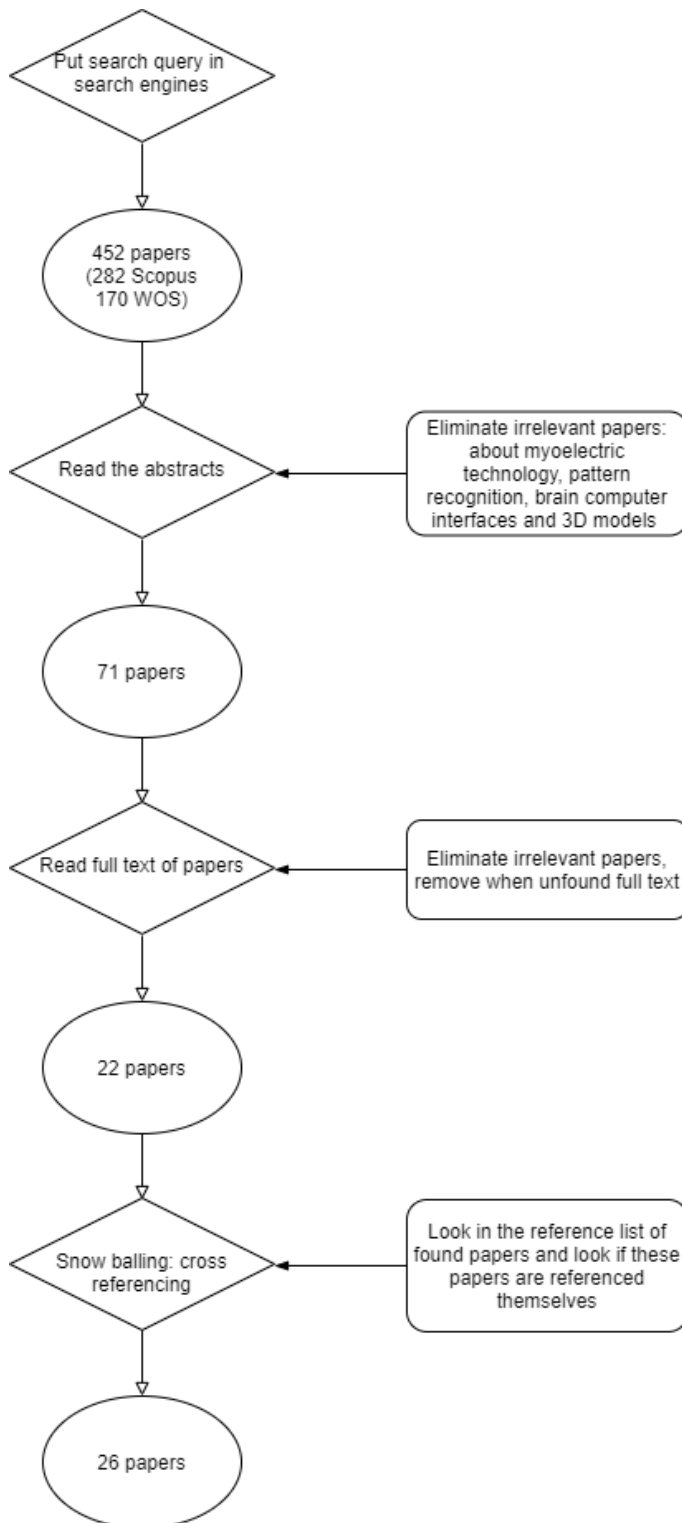


Figure 6: Schematic overview of search process